Mineralogical Magazine, June 2018, Vol. 82(3), pp. 491–514

Placer platinum-group minerals in the Shetland ophiolite complex derived from anomalously enriched podiform chromitites

Hazel M. Prichard[1], Saioa Suárez[1,2,*], Peter C. Fisher[1], Robert D. Knight[1] and John S. Watson[3]

[1] School of Earth and Ocean Sciences, Cardiff University, Main College, Park Place, Cardiff, CF10 3AT, UK
[2] Department of Mineralogy and Petrology, UPV/EHU, 48940 Leioa & Ikerbasque, 48011 Bilbao, Spain
[3] Open University, Department of Environment, Earth and Ecosystems, Walton Hall, Milton Keynes, Buckinghamshire, MK7 6AA, UK

[*Received 21 August 2017; Accepted 17 December 2017; Associate Editor: Brian O'Driscoll*]

ABSTRACT

Highly anomalous platinum-group element (PGE) concentrations in the podiform chromitites at the Cliff and Harold's Grave localities in the Shetland ophiolite complex have been well documented previously. The focus of this study is alluvial platinum-group minerals (PGM) located in small streams that drain from the PGE-rich chromitites. The placer PGM assemblage at Cliff is dominated by Pt-arsenides (64%) and Pd-antimonides (17%), with less irarsite–hollingworthite (11%) and minor Pd-sulfides, Pt–Pd–Cu and Pt–Fe alloys and laurite. Gold also occurs with the PGM. Alluvial PGM have average sizes of 20 μm × 60 μm, with sperrylite the largest grain identified at 110 μm in diameter, matching the range reported for the primary PGM in the source rocks. The placer assemblage contains more Pt-bearing and less Pd-bearing PGM compared with the rocks. The more resistant sperrylite and irarsite–hollingworthite grains which are often euhedral become more rounded further downstream whereas the less resistant Pd-antimonides which are commonly subhedral may become striated and etched. Less stable phases such as Pt- and Pd-oxides and other Ni-Cu-bearing phases located in the rocks (i.e. Ru-pentlandite, PtCu, Pd–Cu alloy) are absent in the placer assemblage. Also the scarce PGM (PdHg, Rh- and Ir-Sb) and Os in the rocks are absent. At Harold's Grave only three alluvial PGM (laurite, Ir, Os) and Au were recovered reflecting the limited release of IPGM from chromite grains in the rocks. In this cold climate with high rainfall, where erosion dominates over weathering, the PGM appear to have been derived directly from the erosion of the adjacent PGE-rich source rocks and there is little evidence of *in situ* growth of any newly formed PGM. Only the presence of dendritic pure Au and Pd-, Cu-bearing Au covers on the surface of primary minerals may indicate some local reprecipitation of these metals in the surficial conditions.

Keywords: Shetland ophiolite complex, Cliff, Harold's Grave, alluvial concentrates, platinum-group minerals, platinum-group elements.

Introduction

There are many examples of placer PGM around the world as summarized in Cabri *et al.* (1996) and Weiser (2002). Placer PGM exhibit variable shapes, commonly form flakes or are rounded or knobbly, and more than 90% of placer PGM are alloys of Pt–Fe and Os–Ir–Ru–Pt. Ophiolitic placer PGM tend to be dominated by Os–Ir–Ru alloys (Cabri *et al.*, 1996).

There is a long standing debate about whether placer PGM erode mechanically from PGE-bearing rocks or whether they grow *in situ* in stream banks

*Email: saioa.suarez@ehu.es
https://doi.org/10.1180/minmag.2017.081.099

This paper is published as part of a thematic set in memory of Professor Hazel M. Prichard

draining from PGE-bearing sources. One of the main lines of evidence for mechanical erosion comes from PGM nuggets that contain inclusions of igneous silicates and exotic PGM that may have been preserved in the matrix of the nuggets. Commonly, placer nuggets are much bigger than the PGM in the source rocks. The argument here is that large PGM in the streams represent the few large PGM concentrated from extensive erosion of the host rocks (Cabri and Harris, 1975) and are overlooked in geochemical and petrological surveys. The alternative view is that placer nuggets may grow *in situ* in streams. Destruction of PGM by weathering and erosion of the host rocks would liberate the PGE, which may travel downstream in solution and re-precipitate due to changes in the geochemistry of the PGE-bearing solutions (e.g. Bowles, 1986; Bowles *et al*., 2000). PGM in the host rocks often show evidence of being broken down and oxidized as they weather (Bowles *et al*., 2017), thus destroying the PGM for later re-precipitation in the streams. The secondary precipitation of placer PGM has been evidenced by reworking and concentric growths (e.g. Cabral *et al*., 2009; Zaccarini *et al*., 2013), or by delicate arrangements of PGM (e.g. Bowles *et al*., 2018) inconsistent with pervasive mechanical and hydraulic erosion of the grains.

Podiform chromitites in ophiolite complexes are typically enriched in IPGE (Ir, Ru, Os) over PPGE (Pt, Pd, Rh) and are characterized by Ru–Os–Ir-dominant PGM (IPGM), mainly laurite–erlichmanite (RuS_2–OsS_2), irarsite (IrAsS) and Os–Ir–Ru alloys. Relevant examples are compiled, for example, in Prichard and Brough (2009) and O'Driscoll and González-Jiménez (2016). Some other ophiolitic chromitites are however significantly enriched in PPGE and contain Pt-, Pd- and Rh-bearing minerals (PPGM), e.g. sperrylite ($PtAs_2$), stibiopalladinite (Pd_5Sb_2), isoferroplatinum (Pt_3Fe), cooperite–braggite (PtS–PdS) and Pt–Pd–Rh±base-metal alloys (González-Jiménez *et al*., 2014). Some well known examples are chromitites from Thetford Mines (Corrivaux and Laflamme, 1990) and Newfoundland (Baie Verte Peninsula; Escayola *et al*., 2011) in Canada, Leka in Norway (Pedersen *et al*., 1993), Cabo Ortegal in Spain (Moreno *et al*., 1999, 2001), Bragança in Portugal (Bridges *et al*., 1993), Albanian ophiolites (Ohnenstetter *et al*., 1999), Pindos in Greece (Grammatikopoulos *et al*., 2007; Prichard *et al*., 2008*a*), Berit in Turkey (Kozlu *et al*., 2014), Al'Ays in Saudi Arabia (Prichard *et al*., 2008*b*), Acoje in the Philippines (Bacuta *et al*., 1988; Orberger *et al*., 1988) and Pirogues in New Caledonia (Augé *et al*., 1998).

The Shetland ophiolite situated on Unst, the most northerly of the Shetland Islands, northeast of Mainland Scotland, was one of the first ophiolite complexes found to contain chromitites enriched in both IPGM and PPGM, with all six PGE being present at ppb or ppm levels (Prichard *et al*., 1986). The history of their discovery is described in Brough *et al*. (2015). Prichard *et al*. (2008*b*) and Prichard and Brough (2009) concluded that the PPGE-rich chromitites in ophiolites formed from magmas that were close to sulfide liquid saturation, resulting in the local accumulation of traces of strongly PGE-enriched sulfide liquid.

The Shetland ophiolite consists of mantle harzburgite overlain by crustal dunite, wehrlite, pyroxenite and gabbro, with a few dykes intruded into the gabbro at the top of the sequence (Fig. 1) (Prichard, 1985; Flinn, 1985). The mantle and crustal ultramafics contain disseminated chromite and there are a number of podiform chromitites in the mantle that are surrounded by an envelope of dunite enclosed in harzburgite. Not all of these pods are enriched in PGE with concentrations of only 10–100 ppb. The exceptions are localities at Cliff and Harold's Grave where enrichment is at ppm levels (up to ~58 and 14 ppm total PGE, respectively). The Cliff locality is enriched in all six PGE and is the main focus of this study whereas the Harold's Grave locality is enriched in IPGE (Prichard and Brough, 2009).

There have been a number of studies of the PGM in the Shetland ophiolite. Generally the PGM in the chromitites are characterized by euhedral Os-Ir-bearing laurite included within the chromite grains and Os-Ir-barren laurite of irregular shape where the laurite is in contact with the serpentine interstitial to the chromite grains. This interstitial laurite is often accompanied by native Os, irarsite and ruthenian pentlandite (Prichard *et al*., 1986; Tarkian and Prichard, 1987; Prichard *et al*., 1994). Occasional composite grains consisting of more varied PGM do, however, occur as for example in the chromitite pod at Nikkavord North, South Cliff, which consists of laurite, irarsite, hollingworthite (RhAsS), ruthenian pentlandite, Ni-Rh antimonide and native Os (Prichard *et al*., 1986). The PGM assemblage in the overlying crustal dunite, wehrlite and pyroxenite sequence contain IPGM in discontinuous chromite layers and PPGM in adjacent sulfide-bearing dunite including Pt-, Pd-rich stibiopalladinite, geversite ($PtSb_2$), genkinite ($(Pt,Pd)_4Sb_3$), Pt–Fe–Cu alloys and Pt- and Pd-oxides

https://doi.org/10.1180/minmag.2017.081.099 Published online by Cambridge University Press

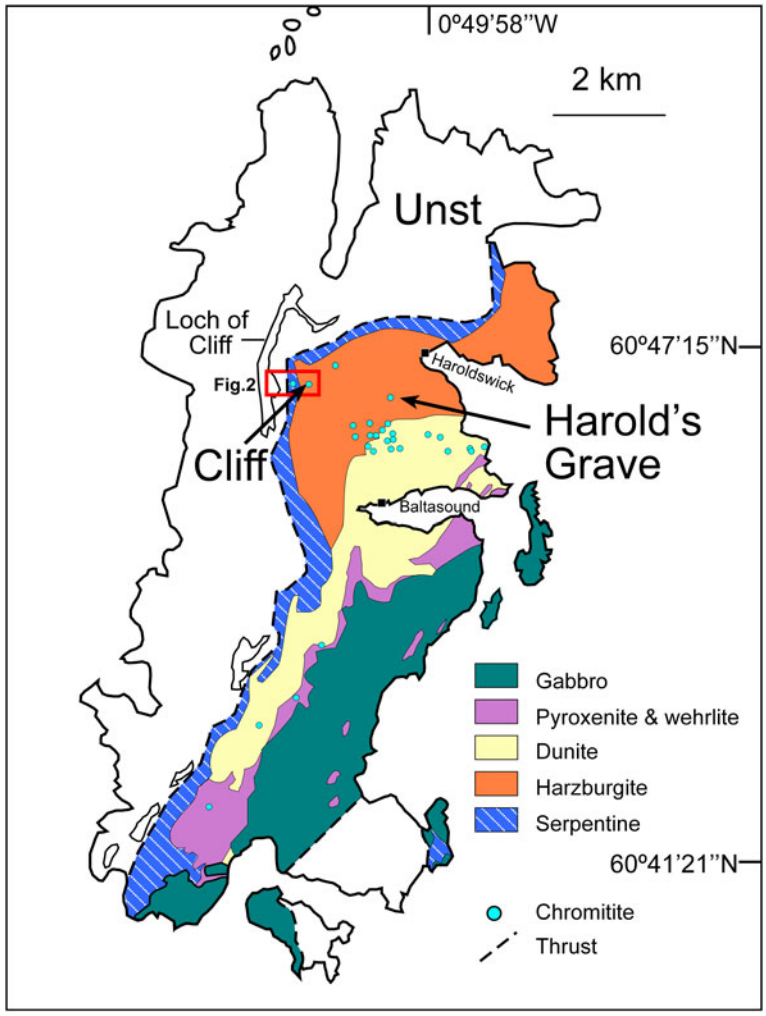

FIG. 1. Geological map showing the locations of the Cliff and Harold's Grave podiform chromitites in the Shetland ophiolite complex.

and ochres, which are low-reflectance minerals formed during the alteration of earlier PGM (Prichard *et al.*, 1994). The wehrlite contains a mineral assemblage formed from a more fractionated magma consisting of Pd–Cu sulfide and Pd–Pb alloys ±Pt and ±Au in unaltered clinopyroxenite, with Pt and Pd arsenides, antimonides and tellurides in adjacent serpentine (Prichard *et al.*, 1994). The PGM located in different stratigraphic levels and in the different chromitite pods within the mantle have been summarized in Prichard *et al.* (1994).

The present study focuses on the two PGE-rich localities of the Shetland ophiolite, Cliff and Harold's Grave. Both are disused chromite quarries located in the north of the ophiolite and consist of several *en echelon* chromitites (also including chromite-rich lenses with >10% chrome-spinel, normally 50–90%) enclosed by a dunite envelope in mantle harzburgite. Cliff is near the basal thrust (Fig. 2) and has a dunite envelope smaller than Harold's Grave. Chromitite lenses at both localities are up to 10 m long and 1 m wide (Prichard *et al.*, 1988). PGM in the Cliff and Harold's Grave chromitites are described in Prichard and Tarkian (1988) and Tarkian and Prichard (1987). These authors observed that IPGM are often enclosed in

https://doi.org/10.1180/minmag.2017.081.099 Published online by Cambridge University Press

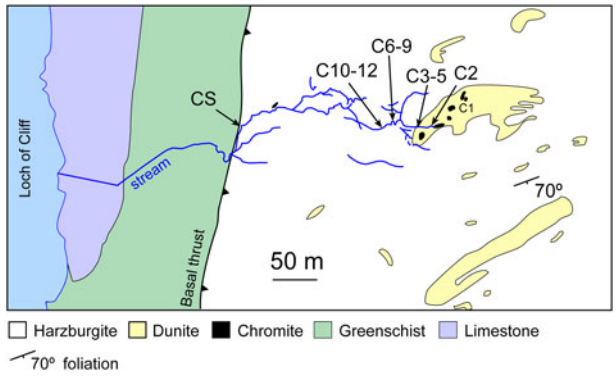

FIG. 2. Geological map of inset in Fig. 1 showing the Cliff chromitites and associated streams in detail. Sampling sites C2–12 and CS are labelled.

chromite whereas PPGE-bearing PGM occur within the serpentinized silicate matrix and are predominantly interstitial to the chromite grains.

PGM at Harold's Grave are dominated by laurite, ruthenian pentlandite, native Os and irarsite often rimmed by hollingworthite. Other minerals recorded include genkinite, hongshiite (PtCu), stibiopalladinite and unnamed Rh–Sb–S and Rh–Ni–Sb phases (Prichard and Tarkian, 1988). Recent studies reveal up to five generations of PGM in these chromitites (Prichard *et al.*, 2017). In contrast, the PGM in the rocks at Cliff are PPGM dominated. A PPGM assemblage occurs in sulfide-bearing dunites adjacent to the chromitites which contain IPGM. The very enriched PPGM-bearing dunite with disseminated chromite is thought to have been hydrothermally upgraded during the introduction of As and Sb, at a late stage as the ophiolite was emplaced (Prichard and Lord, 1993; Lord *et al.*, 1994). In this alteration assemblage all six PGE form PGM in chromite-rich dunites at Cliff. The PGM consist of sperrylite, Pd-antimonides, members of the irarsite–hollingworthite solid solution series, Pt–Pd–Au–Cu alloys, laurite, native Os, potarite (PdHg) and Pt- and Pd-oxides, with PGM diameters up to 30 μm, all accompanied by ruthenian pentlandite. Other studies have been undertaken on the Cliff PGM as for example by Derbyshire *et al.* (2012) who located mainly sperrylite.

The aim of this investigation was to examine the streams draining the Cliff and Harold's Grave sites to characterize the placer PGM present and assess their genesis. The placer PGM are compared to the primary PGM in the source rocks, and variations in the former with increasing distance from the source rocks are also assessed. This study shows for the first time the PGM in the streams draining the Shetland ophiolite and contributes to the increasing knowledge base regarding whether alluvial PGM are mechanically eroded from their source rocks, or whether they precipitate *in situ* as a result of chemical weathering.

Methods

A small network of streams with a maximum width of 0.5 m drains the ponds in the disused chromite quarries at Cliff. These then coalesce to discharge into the Loch of Cliff, 400 m to the west of the Cliff quarries (Fig. 2). Rock samples were taken at the quarries and samples of sediments were collected from the streams at four separate locations (Figs 2 and 3; Table 1) and panned on site in a plastic pool. Four samples (C2–C5) were taken from the first location, at the commencement of the stream from the quarry pond. Sample C2 was taken at the immediate exit of the pond whereas samples C3–C5 were within 5 m of the Cliff quarries. A further four samples (C6–C9) were collected from the second location consisting of meanders 20–50 m downstream of the quarries. Another three samples (C10–C12) were taken downstream within 20–30 m of the exit of the meander zone and after a moderate increase in the slope gradient. Lastly, samples were collected from the stream as it plunged over the basal thrust of the ophiolite (CS).

Sampling at Harold's Grave was conducted over a sloping E–W section spanning ~20 m along a stream draining outcrops of dunite cut by discontinuous layers of chromitite (Table 2). The section starts below a disused PGE-rich quarry and sampling included ten sites separated by three natural ponds, the first two aligned at the beginning

https://doi.org/10.1180/minmag.2017.081.099 Published online by Cambridge University Press

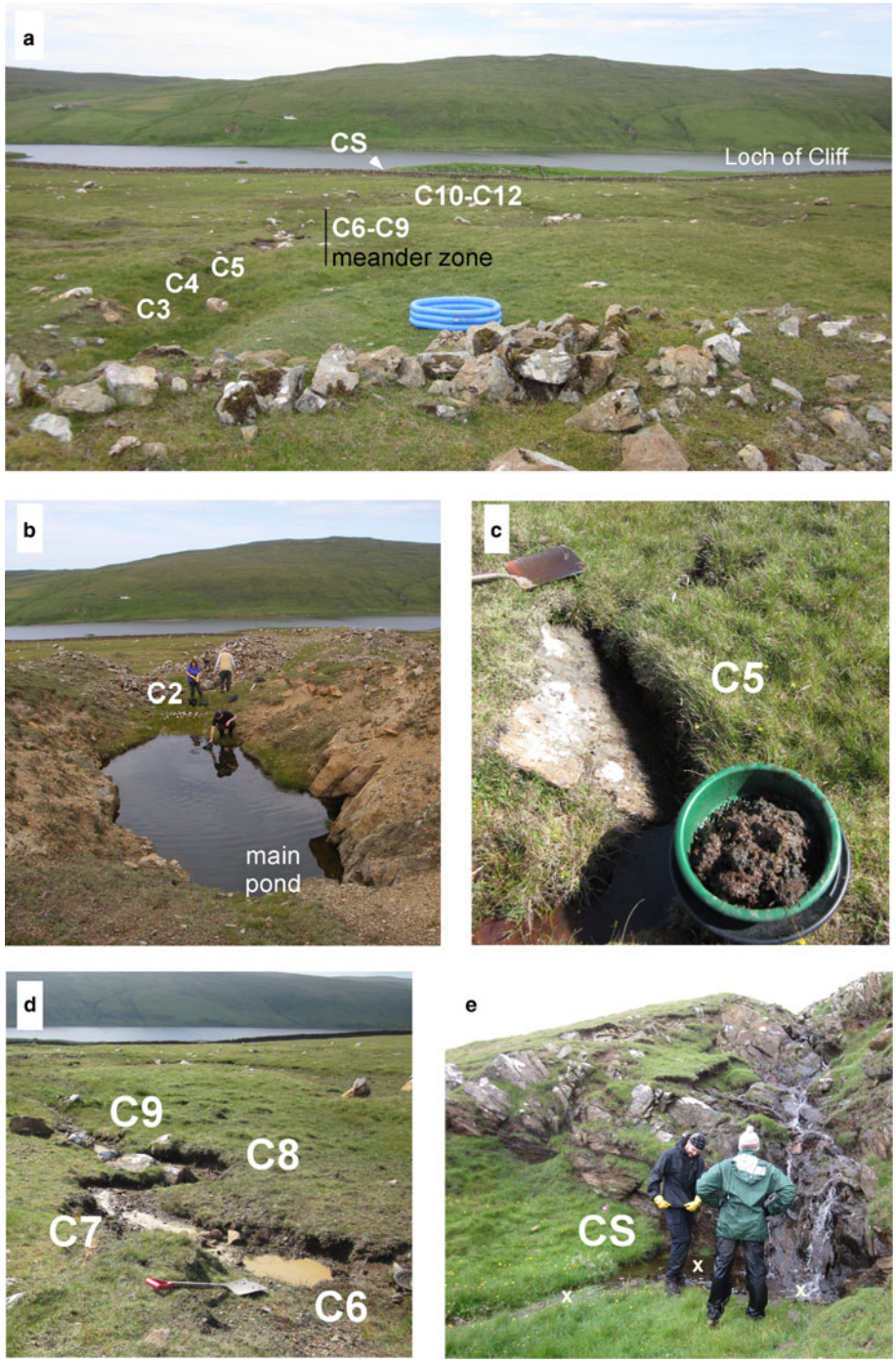

FIG. 3. Sampling sites at Cliff. (*a*) General view looking west from the disused chromitite pits showing all sampling sites. (*b*) View of the pond at the pit and of sample site C2. (*c*) Sample site C5. (*d*) View of the stream meanders and sample sites C6 to C9. (*e*) Sample site CS where the streams amalgamate and plunge over the basal thrust of the ophiolite; the site nearest to the Loch of Cliff.

https://doi.org/10.1180/minmag.2017.081.099 Published online by Cambridge University Press

TABLE 1. Types of PGM in the Cliff chromitites and alluvial PGM recovered from the associated streams.

PGM, Au	Composition	No. grains	%	Size (μm)	
				Min	Max
1) Source rock*					
Sperrylite	$(Pt,Fe)(As,Sb)_2$	37	38.1	4	20
Hongshiite	PtCu+(Ni–Cu)	1	1.0	4	5
Pt-alloys	Pt–Pd–Au–Cu; Pd–Cu	4	4.1	2	8
Pd-antimonide	Pd_5Sb_2–$Pd_{11}Sb_4$	24	24.7	4	17
Ni-(Ru)-sulfide	$(Ni,Fe,Ru,Cr)_9S_8$	4	4.1	10	30
Potarite	PdHg	1	1.0	2	3
Irarsite	IrAsS	9	9.3	10	60
Hollingworthite	RhAsS	7	7.2	7	19
Rh-antimonide	Rh–Sb–S	1	1.0	3	4
Laurite	RuS_2	3	3.1	10	27
Osmium	Os	1	1.0	2	5
Gold	Au–(Pd), Au–Cu	5	5.2	3	4
Total		97	100	5	17
2) Exit pond (samples C3─C5)					
Sperrylite	$(Pt,Rh)(As,Sb)_2$	14	56.0	14	92
Pt-alloys	Pt–Pd–Cu alloy	1	4.0	10	50
Pd-antimonide	$(Pd,Cu)_5$ $(Sb,S, As)_2$	5	20.0	19	90
Pd-sulfide	$Pd_{16}(S,As)_7$	2	8.0	8	20
Irarsite	(Ir,Rh)AsS	1	4.0	27	60
Hollingworthite	(Rh,Pt)AsS	1	4.0	10	50
Gold	Au–(Ag)	1	4.0	58	60
Total		25	100	21	60
3) Meander (samples C6─C9)					
Sperrylite	$(Pt,Rh)(As,Sb)_2$	42	60.9	30	110
Pt-alloys	Pt (Fe,Ni,Cu)	1	1.4	15	20
Pd-antimonide	$(Pd,Fe,Cu)_5$ $(Sb,As,S)_2$	9	13.0	34	85
Pd-arsenide	$(Pd,Fe,Ni)_2$ (As,S)	1	1.4	15	20
Pd-sulfide	(Pd,Pt,Ni,Fe)S	2	2.9	13	70
Irarsite	(Ir,Rh,Pt)AsS	4	5.8	44	63
Hollingworthite	(Rh,Pt)AsS	3	4.3	10	80
Laurite	RuS_2	1	1.4	20	45
Gold	Au–(Ag); Au–(Cu,Pt,Pd)	6	8.7	31	48
Total		69	100	24	60
4) Exit meander (samples C10─C11)					
Sperrylite	$PtAs_2$	13	61.9	22	106
Pt-alloys	$Pt_3(Fe,Ni,Cu)$	1	4.8	57	62
Pd-antimonide	$(Pd,Cu)_5(Sb,S,As)_2$	4	19.0	36	103
Irarsite	(Ir,Rh)AsS	1	4.8	47	84
Hollingworthite	(Rh,Os,Pt)AsS	1	4.8	64	80
Gold	Au–(Pd)	1	4.8	5	20
Total		21	100	39	76
5) Waterfall (basal thrust, sample CS)					
Laurite	$(Ru,Os)(S,As)_2$	1	100	10	32

*PGM in the source rocks from Prichard *et al.* (1986) and Prichard and Tarkian (1988) for comparison purposes.

https://doi.org/10.1180/minmag.2017.081.099 Published online by Cambridge University Press

TABLE 2. Types of PGM in the Harold's Grave chromitites and alluvial PGM recovered from the associated streams.

PGM	Composition	No. grains	%	Size (μm) Min	Max
1) Source rock*					
Osmium	Os	49	47.6	2	5
Laurite	RuS_2	30	29.1	10	250
Ni-(Ru)-sulfide	$(Ni,Fe,Ru,Cr)_9S_8$	4	3.9	10	30
Irarsite	IrAsS	5	4.9	10	60
Ir-antimonide	Ir–Sb–S	1	1.0	6	6
Hollingworthite	RhAsS	4	3.9	7	20
Rh-antimonide	Rh–Sb–S	3	2.9	2	4
	Rh–Ni–Sb	1	1.0	2	6
Hongshiite	PtCu	1	1.0	4	5
Pt-alloys	Pt–Pd–Cu	1	1.0	5	6
Genkinite	$(Pt,Pd)_4Sb_3$	2	1.9	2	12
Pd-antimonide	Pd_5Sb_2–$Pd_{11}Sb_4$	2	1.9	3	17
Total		103	100	5	35
2) Stream					
Laurite (HG7)	RuS_2	1	14.3	35	50
Iridium (HG7)	Ir–(Fe > S,As)	1	14.3	20	20
Osmium (HG10)	Os–(Ir–Ru)	1	14.3	30	60
Gold (HG1-2-7)	Au–Ag, Au–Cu	4	57.1	149	224
Total		7	100	59	89

*PGM in the rocks are from Tarkian and Prichard (1987).

of the section and the last one situated further down slope. The first five samples (HG1─HG5) were taken from the entrance and exit of the first two ponds. This area is covered largely by vegetation; it has a 10 cm topsoil with a high concentration of organic matter followed by a subsoil layer of significantly weathered rock. The soil produced negligible heavy concentrates and holes were excavated to a depth of 15–20 cm to obtain samples. The next four samples (HG6─HG9) were collected from a site with more outcrop of fractured dunite following a strong break of slope with increasing gradient. The last sample (HG10) was taken from the exit of the most distal pond, where the soil layer becomes thicker again. Overall, the dense fraction recovered from sampling sites at Harold's Grave was much smaller than that recovered from Cliff.

Panned size fractions below 150 μm were examined for precious-metal minerals and PGM using a Cambridge Instruments (ZEISS NTS) S360 scanning electron microscope (SEM), coupled to an Oxford Instruments INCA energy plus energy dispersive X-ray analytical system (EDX) at Cardiff University. Qualitative analyses were obtained of the mineral surfaces, and polished blocks were utilized for fully quantitative analyses (Table 3). Operating conditions for the quantitative analyses consisted of a 20 kV accelerating voltage, 1 nA beam current and fixed beam size (~10–15 nm), with a live-time of 50 s for EDX. A cobalt reference standard was regularly analysed, in order to check for any drift in the analytical conditions. A comprehensive set of standards obtained from MicroAnalysis Consultants Ltd. (St Ives, Cambridgeshire) was used to calibrate the EDX analyser.

Results

Alluvial PGM at Cliff

A total of 108 PGM and 8 grains of gold have been identified in samples C3–C11 and CS collected from the streams at Cliff (Fig. 4*a*, Table 1). The PGM assemblage consists mainly of sperrylite (69

https://doi.org/10.1180/minmag.2017.081.099 Published online by Cambridge University Press

TABLE 3. Results from quantitative EDX analyses of alluvial PGM from Cliff.

Analysis	1	2	3	4	5	6	7	8	9	10	11	12	13
Sample	C3	C5	C6	C9	C4	C6	C10	C6	C9	C5	C6	C10	C6
Wt.%													
Pt	56.25	55.04	54.50	52.97					13.79	21.99		77.29	
Pd					63.20	64.13	63.78						
Rh	0.47		1.24	1.11				6.15	9.56	7.84			
Ir								55.78	36.64	20.78			
Ru		0.99	0.68	1.41						8.93	22.00		
Os											37.44		
Au													75.69
Ag													25.40
Cu					4.00	2.73	3.61					5.42	
Ni						0.60	0.59					4.72	
Fe												12.11	
S		0.32	0.49	1.23				12.95	11.56	11.95	13.35		
As	42.12	41.20	42.25	40.26				25.78	29.91	29.01	30.95		
Sb	1.23	2.29	0.92	2.86	31.80	31.89	32.49						
Total	100.07	99.84	100.08	99.84	99.00	99.35	100.47	100.66	101.47	100.50	103.73	99.54	101.1
At.%													
Pt	33.32	32.41	31.57	30.32					6.35	9.84		50.88	
Pd					64.70	65.67	64.24						
Rh	0.53		1.37	1.21				5.44	8.34	6.66			
Ir								26.43	17.11	9.44			
Ru		1.12	0.76	1.56						7.71	17.50		
Os											15.83		
Au													62.01
Ag													37.99
Cu					6.85	4.68	6.08					10.95	
Ni						1.12	1.08					10.32	
Fe												27.85	
S		1.14	1.71	4.28				36.79	32.37	32.54	33.46		
As	64.99	63.17	63.73	60.01				31.34	35.83	33.81	33.21		
Sb	1.16	2.16	0.86	2.62	28.45	28.54	28.60						

Analysis:

Sperrylite
[1] $(Pt, Rh)_{1.02}(As,Sb)_{1.98}$
[2] $(Pt,Ru)_{1.01}(As,S,Sb)_{1.99}$
[3] $(Pt, Rh,Ru)_{1.01}(As,Sb,S)_{1.99}$
[4] $(Pt,Rh,Ru)_{0.99}(As,S,Sb)_{2.01}$

Pd-antimonide
[5] $(Pd,Cu)_{5.01}Sb_{1.99}$
[6] $(Pd,Cu,Ni,Fe)_5Sb_2$
[7] $(Pd,Cu,Ni)_5Sb_2$

Irarsite
[8] $(Ir,Rh)_{0.96}As_{0.94}S_{1.10}$
[9] $(Ir,Rh,Pt)_{0.95}As_{1.08}S_{0.97}$

Platarsite
[10] $(Pt,Ir,Ru,Rh)_{1.01}As_{1.01}S_{0.98}$

Ruarsite
[11] $(Ru_{0.52}Os_{0.47})AsS$

Pt-alloy
[12] $Pt_{1.02}(Fe_{0.56}Cu_{0.22}Ni_{0.20})_{0.98}$

Electrum
[13] $Au_{0.62}Ag_{0.38}$

grains; 64% abundance), Pd-antimonides (18 grains; 17%) and members of the irarsite–hollingworthite solid-solution series (11 grains; 11%). Less abundant phases are Pd-sulfides (4 grains; 4%) and Pt-alloys, Pd-arsenide and laurite (6 grains in total; 6%). These PGM range in size from 8–110 μm and consist of single minerals as well as composite grains. The placer PGM reflect those observed in the source rocks, but exhibit less variety (Fig. 4*a*, Table 1). Quantitative analyses of polished surfaces of the typical PGM have been completed (Table 3).

https://doi.org/10.1180/minmag.2017.081.099 Published online by Cambridge University Press

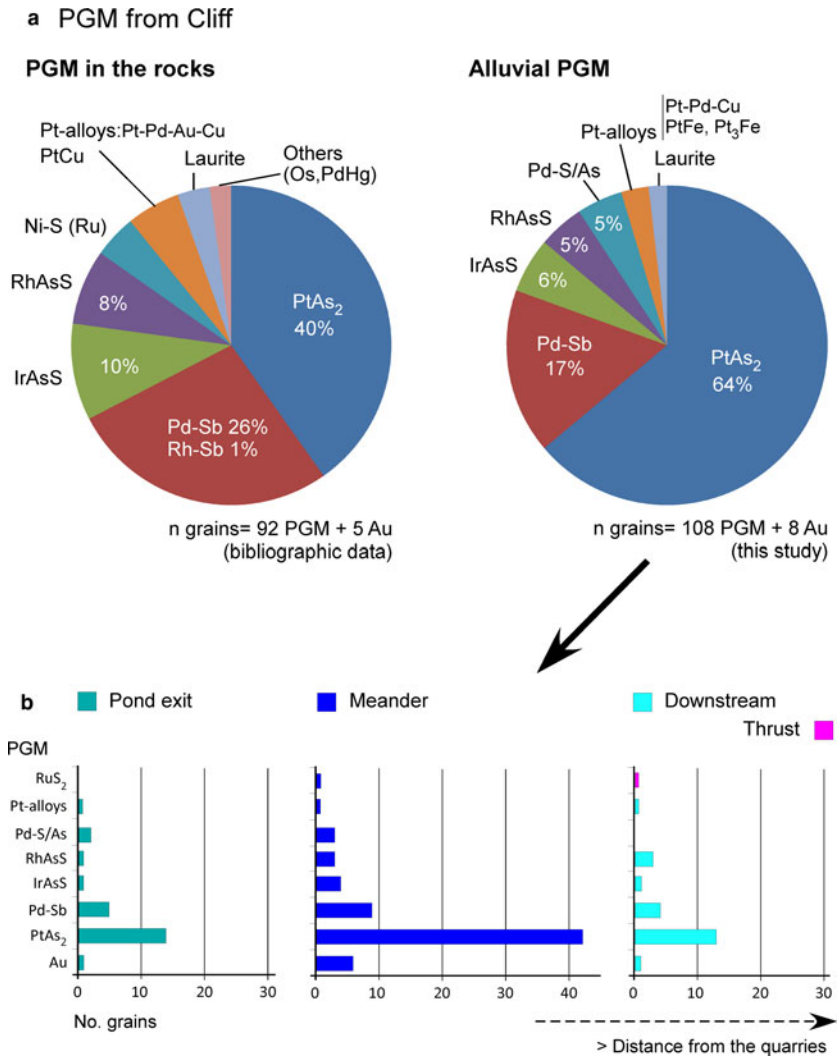

FIG. 4. (*a*) Pie diagrams showing the different PGM located in the chromite-rich rocks from Cliff (illustrative data, from Prichard *et al*. 1986 and Prichard and Tarkian, 1988), and in the streams panned in this study. (*b*) Bar graphs showing the number of alluvial PGM recovered with increasing distance from the Cliff quarries: pond exit zone (samples C3–C5), following meander zone (samples C6–C9), exit of the meander downstream (samples C10–11) and basal thrust (sample CS). See Table 1 for more detail.

Alluvial PGM in the streams at Cliff occur only within the first 100–150 m from the disused quarries (Fig. 2; Fig. 4*b*). Of the 108 PGM grains recovered, 22% are from the exit of the main pond close to the quarries, 58% are from the meander zone ~50 m away from the quarries, and 19% come from downstream of the meander exit, ~100 m away. However, only one PGM grain was recovered further downstream, where the stream plunges over the basal thrust. The type, abundance and size of the alluvial PGM do not vary significantly downstream (Table 1, Fig. 4*b*). Sperrylite, Pd-antimonides and sulfarsenides together with Pt-alloys and gold occur all along the stream. Palladium-sulfides and -arsenides persist closer to the quarries but are not present downstream and laurite, although scarce, appears furthest from the source (Fig. 4*b*). The main PGM recovered from the streams at Cliff are described next.

https://doi.org/10.1180/minmag.2017.081.099 Published online by Cambridge University Press

Sperrylite

Sperrylite is the most abundant PGM in the streams draining Cliff. It is commonly euhedral to subhedral and occurs in single cubes, octahedrons or aggregates of cubes that are more or less abraded. Single grains range in size from 15 to 110 μm and aggregates reach up to 100 μm across.

Angular sperrylite is more common close to the Cliff quarries (Fig. 5). This sperrylite is often cracked, with pits and furrows on the surface. It occasionally shows surface structures that may correspond to a cleavage (Fig. 5*a–c*) and it can occur intergrown with silicates preserved from the host rock (Fig. 5*d–e*), possibly chlorite or serpentine. Many grains of sperrylite show a more jagged and altered appearance with extensive pitting of the mineral surfaces (Fig. 5*f–i*). Grains or aggregates of euhedral sperrylite show more abraded edges with increasing distance from the quarries (Fig. 5*j–l*). In fact, ~40% of the sperrylite grains recovered from the streams are subhedral to subrounded (Fig. 6*a–l*) and occur mainly downstream, further from the quarries.

Sperrylite forms composite grains with irarsite (Fig. 7*a–b*) and Pd-antimonides (Fig. 7*c–d*). It also occurs with laurite (Fig. 7*e*) and with the only grain of Pd-arsenide identified (Fig. 7*f*), which attains a composition close to $(Pd,Fe,Ni)_2(As,S)$. Polished sections of sperrylite reveal other mineral associations (Fig. 8). These include: (1) Pt-alloys of the tetraferroplatinum type (PtFe) in elongate grains 40 μm across that are enclosed in broken sperrylite (Fig. 8*a*); (2) ruarsite (RuAsS) at the contact between sperrylite and stibiopalladinite (Fig. 8*b*); (3) platarsite (PtAsS) on the edge of abraded sperrylite (Fig. 8*c*); and (4) Ni-sulfides and -arsenides (millerite (NiS) – godlevskite (Ni_9S_8) and nickeline (NiAs)), which occur as euhedral or elongated inclusions <10 μm long within sperrylite (Fig. 8*d*).

Sperrylite has a regular $PtAs_2$ composition throughout the streams. Occasionally Rh (up to 9 wt.%), and minor amounts of Ru, Pd, Fe or Cu (≤ 2 wt.% each) have been detected. Antimony and S (≤ 4 wt.% each) can replace As (Table 3). This composition is similar to that of sperrylite in the source chromitites, which contain lower but regular Fe (<0.5 wt.%) and Sb concentrations (≤ 3 wt.%) (Prichard and Tarkian, 1988).

Palladium antimonides

Palladium antimonides are the next most abundant PGM. The size of these PGM ranges from 20 to 105 μm in diameter. They are more altered than the sperrylites in the streams and only 23% of the grains recovered preserve a euhedral shape (Fig. 9*a*). This occurs normally close to the quarries, where grains are often broken (Fig. 9*b–c*). Within the meander zone, all the grains show a characteristic fine striation on their surfaces (Fig. 7*c*; Fig. 9*d–g*) denoting a lower resistance in the stream compared to sperrylite. The group of grains located at the exit of the meander zone all show an etched appearance (Fig. 9*h–i*). Polished sections of Pd-antimonide grains are smooth and internal inclusions are not observed. They typically exhibit homogeneous cores surrounded by an external rim of dismembered Pd-antimonide. Internal fractures are also common (Fig. 8*b*).

Pd-antimonides often form composite grains with sperrylite (Fig. 7*c–d*, Fig. 8*b*), Pd-sulfides (Fig. 9*a*) and Pt-alloys consisting of Pt–Pd–Cu (Fig. 9*c*) and PtFe (Fig. 9*e*). The latter is a tetraferroplatinum included within a Pd-antimonide grain (Fig. 9*e*). In some cases, Pd-antimonide occurs with electrum (e.g. Fig. 9*d*) which forms a thin cover along the surface structures of the PGM.

Alluvial Pd-antimonides attain a composition that resembles stibiopalladinite ($Pd_{31}Sb_{12}$–$Pd_{5+x}Sb_{2-x}$, where $x = 0.04$) with some compositions extending towards Pd_5Sb_3, according to ideal Pd–Sb phases of the Pd–Sb–Te system reported by Kim and Chao (1991) (Fig. 10*a*). Analyses of Pd-antimonides yield elevated Cu contents for most of the analysed grains (0–5 wt.% Cu; av. 2.7 wt.%), occasional contents of As (≤ 3.5 wt.%) and Ni (≤ 0.7 wt.%), and rare Fe (≤ 2.7 wt.%) (Table 3). No other PGE have been recorded other than Pt. Similar compositions are reported for Pd-antimonides in the host rocks at Cliff (mertieite-II – stibiopalladinite, Fig. 10*a*), although these contain more Pd, and some Pt up to 0.8 wt.% (Prichard and Tarkian, 1988).

Sulfarsenides

End and intermediate members of the irarsite–hollingworthite–platarsite solid solution series have been located throughout the streams draining Cliff.

Irarsite is the most abundant phase ($n = 6$ grains) and occurs in single or composite grains and aggregates with sizes ranging from 30 to 84 μm in diameter. Irarsite in composite grains can be euhedral (Fig. 7*a–b*) and aggregates with etched surfaces also preserve the euhedral shape of the grains (Fig. 11*a*). More often irarsite occurs as

https://doi.org/10.1180/minmag.2017.081.099 Published online by Cambridge University Press

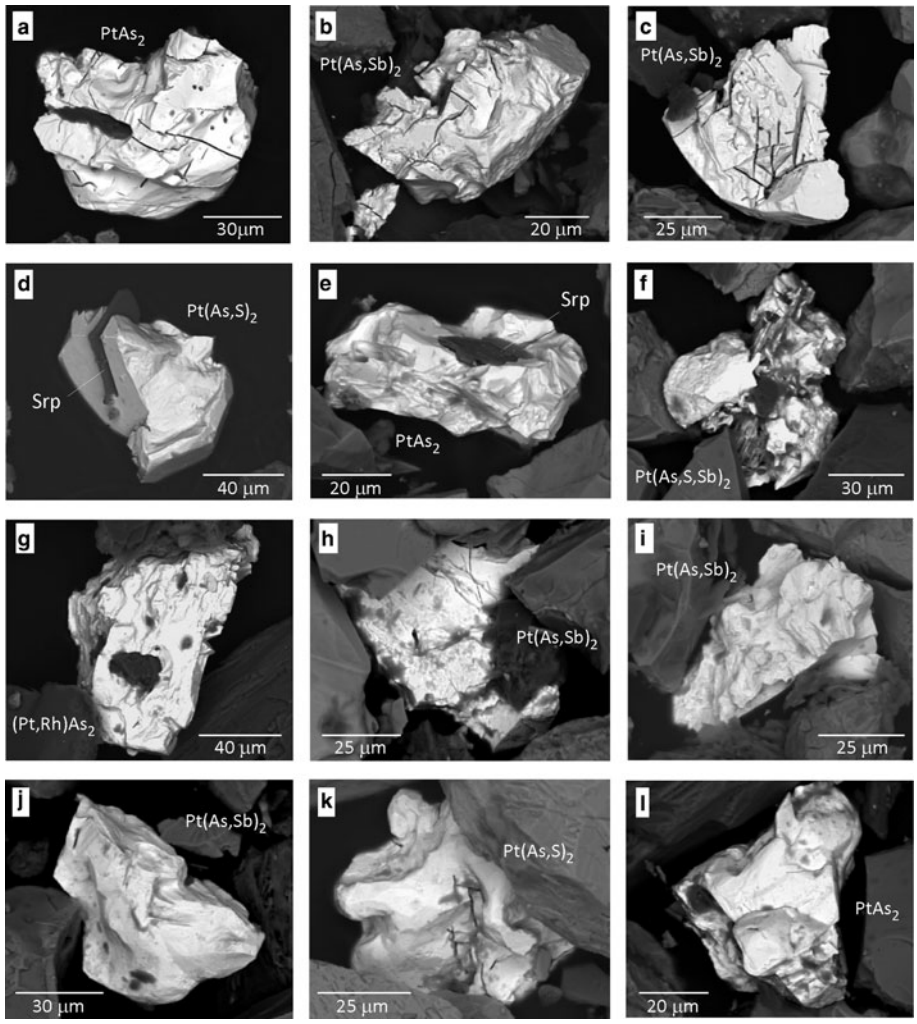

FIG. 5. Back-scattered electron images of sperrylites recovered near the disused quarries from samples C3 to C5. Note the frequent cracks and jagged appearance.

subhedral, etched grains (Fig. 11*b–c*). In two cases it forms composite grains with sperrylite (Fig. 7*a–b*) and in one case with hollingworthite (Fig. 11*c*). Alluvial irarsite shows two compositional trends, one with increasing Rh content and the other with increasing Pt content (Fig. 10*b*). Normally, irarsite attains a (Ir,Rh)AsS composition, with average Rh contents of ~7 wt.% (Table 3). Some Sb is also detected (< 1.5 wt.%). Less often, irarsite contains elevated Pt up to 22 wt.% and Ru up to 10 wt.%. Iridium end-members have not been located in the streams although they are present in the rocks from Cliff (Tarkian and Prichard, 1987; Fig. 10*b*). Exceptionally, one grain of platarsite (PtAsS) and another of ruarsite (RuAsS) have been located in polished sections of the alluvial PGM. Platarsite occurs on the edge of a sperrylite grain (Fig. 8*c*, Table 3). Ruarsite is in a polyphase grain with sperrylite and Pd-antimonide and contains elevated Os up to 37 wt.% (Fig. 8*b*, Table 3). It is of note that irarsite in the rocks from Cliff is unusually Pt poor (Prichard and Tarkian, 1988) whereas Pt-bearing irarsite is observed in the streams (Fig. 10*b*).

Hollingworthite occurs as subhedral grains ($n = 5$) with sizes from 10 to 80 µm across (Fig. 11*c–f*). Two of these are single grains (e.g. Fig. 11*d*) and the other

https://doi.org/10.1180/minmag.2017.081.099 Published online by Cambridge University Press

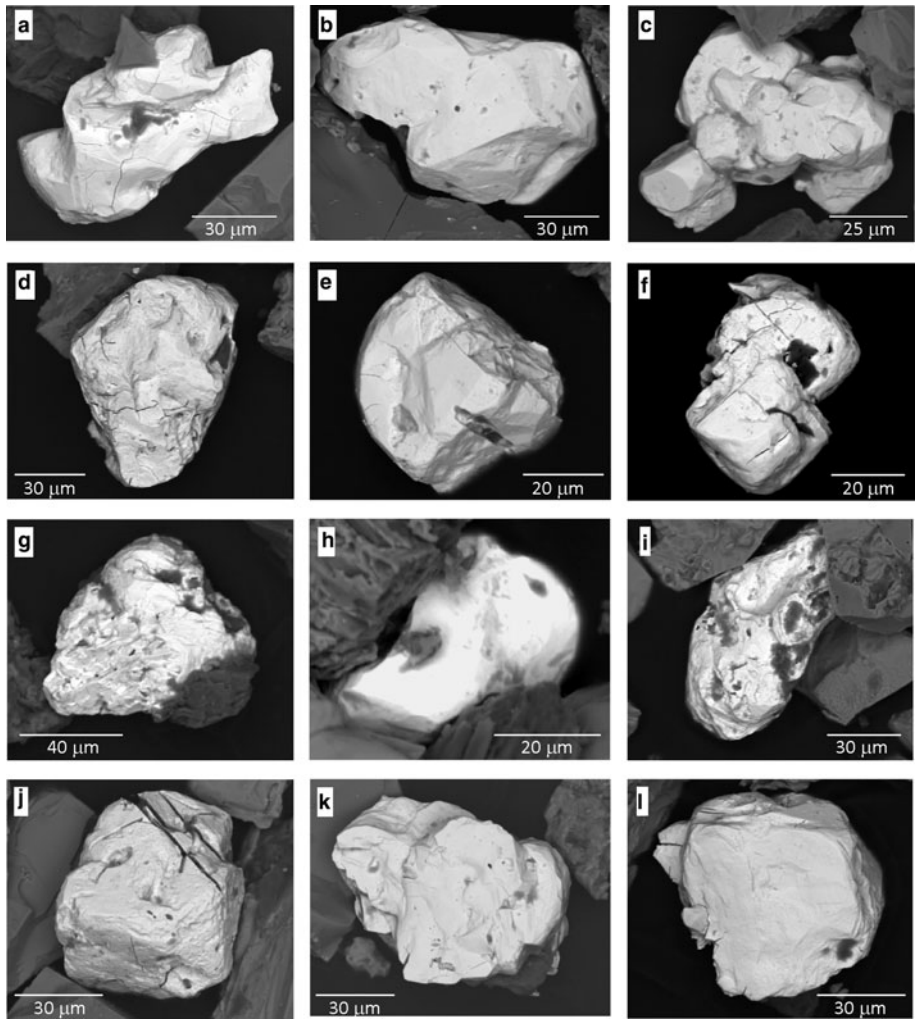

FIG. 6. Back-scattered electron images of sperrylites from further downstream to the disused quarries from samples C6 to C11. Note more rounded appearance than in Fig. 5.

three form composite grains with irarsite (Fig. 11*c*), Pd-antimonide (Fig. 11*e*) or gold (Fig. 11*f*). One grain was identified as end-member hollingworthite (RhAsS, Fig. 11*d*) whereas the others contain Pt (≤ 6 wt.%) and rarely Ir or Os up to 11 wt.% and 6 wt.%, respectively. Similarly to irarsite, hollingworthite contains more Pt in the placers than in the source rocks (Fig. 10*b*).

Less abundant PGM

Palladium sulfides ($n = 4$ grains) occur both as subhedral grains with Pd-antimonides close to the disused quarries at Cliff ($n = 2$ grains, Fig. 9*a*) and as single, broken grains 10–70 µm long in the meander zone. The two grains close to the quarries resemble vasilite in composition $(Pd, Fe, Cu)_{16}$ $(S, As, Sb)_7$ and the grains in the meander resemble vysotskite (Pd, Fe, Ni) (S, As) with low Fe and Ni contents (0–7 wt.% in total).

Platinum alloys ($n = 3$ grains) are different from each other in texture, composition and location along the stream. One grain close to the quarries is a relict euhedral Pt–Pd–Cu alloy ($Pt_{0.78}Pd_{0.15}Cu_{0.07}$), 20 µm across, that occurs in a composite grain with a broken Pd-antimonide (Fig. 9*c*). The second grain is a 50 µm long tetraferroplatinum ($Pt_{1.05}(Fe,Ni,Cu)_{0.95}$) included in a wrinkled Pd-antimonide from

https://doi.org/10.1180/minmag.2017.081.099 Published online by Cambridge University Press

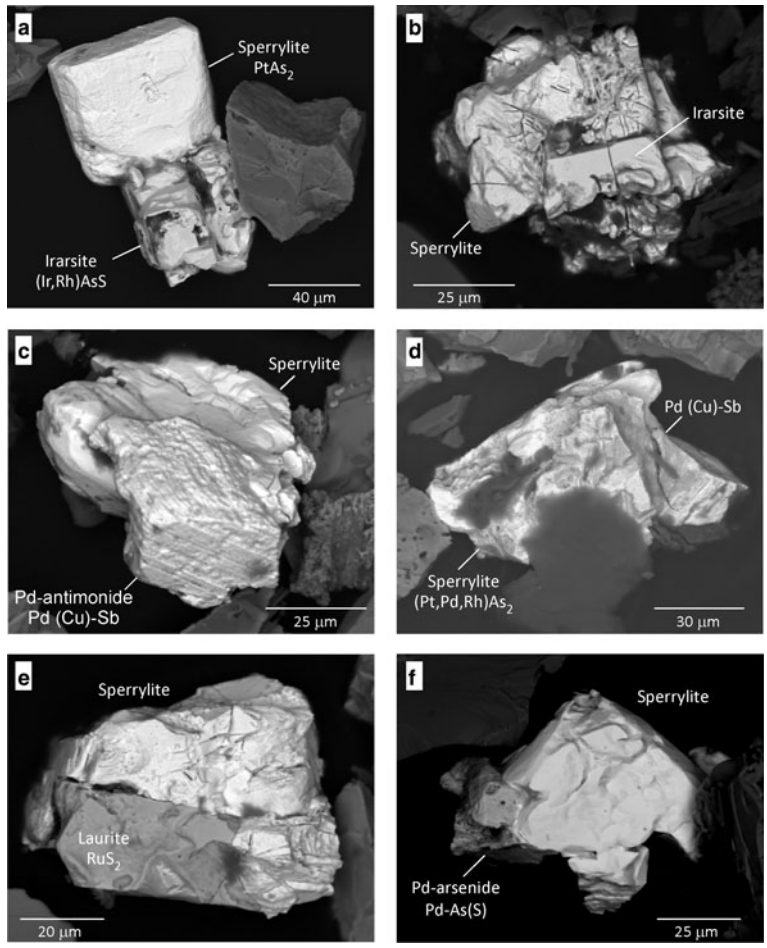

FIG. 7. Back-scattered electron images of composite grains of sperrylite located in the streams from Cliff.

the meander zone (Fig. 9*e*). Another particle of similar composition was also located enclosed by sperrylite in polished sections (Fig. 8*a*). The third grain is a subrounded, single tetraferroplatinum ($Pt_{2.7}(Fe,Cu,Ni)_{1.3}$), 60 µm across, that contains lower Ni and Cu totalling < 5 wt.%. This last grain belongs to sample C10, downstream, after the meander area. Only one analysis of a 5 µm sized Pt–Pd–Cu–Sb alloy from the source chromitites is available in the bibliography (Prichard and Tarkian, 1988) and comparatively, the alluvial Pt–Pd–Cu alloy found is larger and contains more Pt and less Pd (Fig. 10*a*).

Laurite ($n = 2$ grains) is rare in the alluvial assemblage. One grain with Pd-antimonide (Fig. 7*e*) in the meander is euhedral and has a pure composition of RuS_2. The other grain is the only PGM recovered from sample site CS (Fig. 2), the furthest from the Cliff quarries. This is a subhedral single grain with a composition similar to $(Ru,Os)(S,As)_2$, with up to 14 wt.% Os. The presence of both Os-Ir-bearing laurite and Os-free laurite with inclusions of native Os was also noted in the source rocks (Tarkian and Prichard, 1987; Fig. 10*b*). Much of this Os is likely to be derived from the alteration of Os-laurite to pure RuS_2 during serpentinization of the ophiolite (Prichard *et al*., 2017). Both types of laurite remain in the placers.

Other less abundant PGM in the placers include one grain of palladoarsenide (Fig. 7*f*), and one grain of ruarsite and another of platarsite (Fig. 8*b–c*) found only in the polished sections of the alluvial PGM.

https://doi.org/10.1180/minmag.2017.081.099 Published online by Cambridge University Press

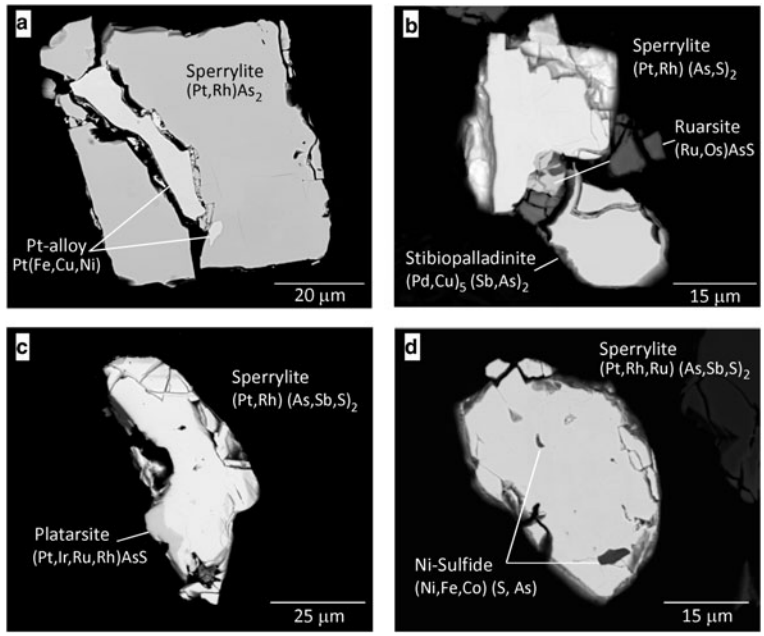

FIG. 8. Back-scattered electron images of polished sections of sperrylite and associated PGM and sulfides. (*a*) Elongate PtFe alloy enclosed in a broken cube of sperrylite. (*b*) Os-bearing ruarsite surrounded by an angular grain of sperrylite at the top and a Cu-bearing stibiopalladinite at the bottom. (*c*) Relicts of platarsite on the edge of an abraded sperrylite. (*d*) Inclusions of millerite (NiS) in sperrylite.

Gold

Eight Au-bearing grains from 30 to 80 μm in diameter have been identified. Five of these occur as single particles of electrum with up to 25 wt.% Ag (Table 3). Only one irregular grain of electrum was recovered close to the Cliff quarries (Fig. 12*a*). Electrum in the meander zone occurs as subhedral pitted grains (Fig. 12*b*), round smooth grains (Fig. 12*c*) and as a porous grain with a delicate structure (Fig. 12*d*). Gold-bearing phases also occur as thin covers on the surfaces of PGM and Au. For example, pitted electrum is observed on the surface of a Pd-antimonide (Fig. 9*d*) and pitted Au-(Cu–Pt–Pd) occurs on the surface of a composite grain of hollingworthite and Au (Fig. 11*f*). Downstream, a Au–Pd cover with up to 2.6 wt.% Pd was observed on a composite grain of Pd-antimonide and sperrylite. Some placer gold particles at Cliff (Fig. 12*a–d*) mimic the textures of the gold grains located in the source rocks, where rounded and porous particles were detected (Fig. 13*a–b*).

Alluvial PGM at Harold's Grave

The results from panning at Harold's Grave were less successful and the source rocks here are dominated by IPGM (Table 2). Platinum-group minerals and gold were recovered from samples HG1, 2, 7 and 10 (Table 2), so they are erratically distributed though the sampling sites. One euhedral composite grain of 40 μm laurite ($Ru_{0.98}S_{2.02}$) with iridium (Ir–Fe–(S,As)), as well as one 60–μm grain of osmium ($Os_{0.9}Ir_{0.06}Ru_{0.04}$) with subhedral shape and pitted edges were recovered from the panned material.

In addition, four Au grains up to 300 μm × 400 μm in size were also recovered. They are all relatively pure in terms of composition. Two grains of Au, both with minor contents of Cu (4–17 wt.%), exhibit the same fine porous texture on their surfaces, although one is euhedral and the other is subrounded. The other two grains (Fig. 12*e–f*) are subhedral and very porous aggregates. They consist of subrounded particles of Au with minor amounts of Ag in composition (6 wt.% on average) and show formations of pure dendritic Au on their surfaces.

Discussion

Examination of the placer PGM derived from the Shetland PGE-rich chromitites at Cliff and Harold's

https://doi.org/10.1180/minmag.2017.081.099 Published online by Cambridge University Press

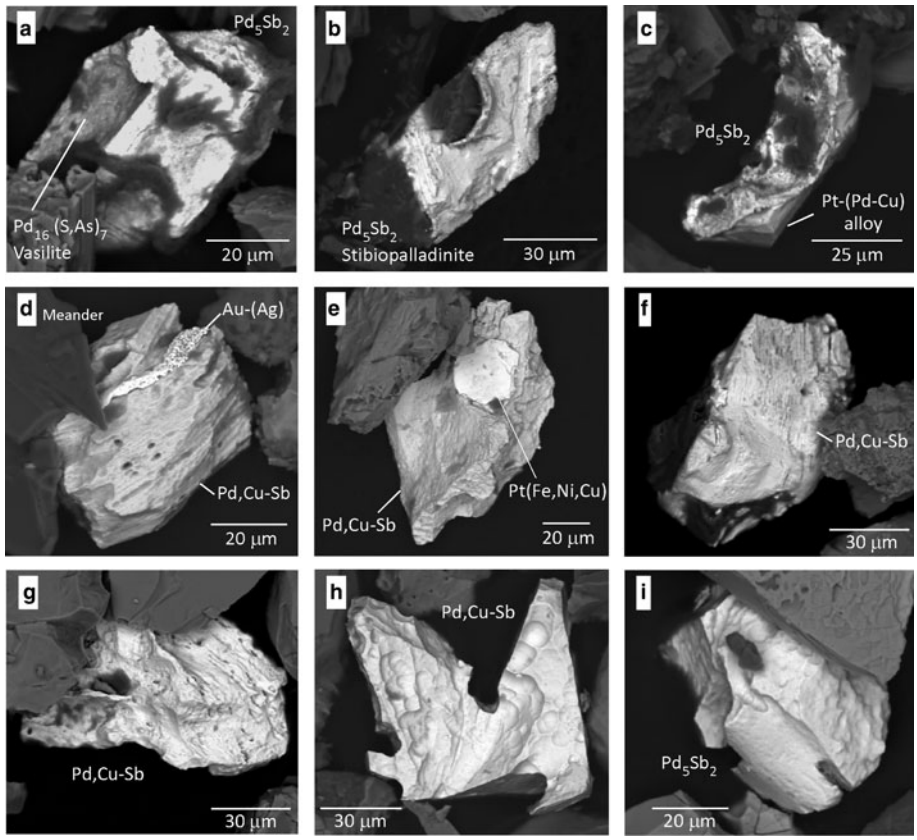

FIG. 9. Back-scattered electron images of Pd-antimonides from the streams draining Cliff. (*a–c*) Pd-antimonides recovered near the disused quarries from samples C3 to C5. (*a*) Angular stibiopalladinite in a composite grain with a Pd-sulfide. (*b*) Stibiopalladinite with a ragged appearance and vast furrows on the surface. (*c*) Relict stibiopalladinite in a composite grain with a euhedral Pt–Pd–Cu alloy. (*d–i*) Pd-antimonides from further downstream to the disused quarries from samples C6 to 11. Note the extensive striation on the grain surfaces in the meander zone (*d–g*, samples C6 to C9) and the etched appearance with concave hollows further downstream (*h–i*, samples C10–C11). Pd-antimonides form composite grains with electrum in (*d*) and with tetraferroplatinum in (*e*).

Grave allows for the comparison between PGM assemblages in the source rocks and streams in order to identify the most relevant modifications of the alluvial minerals and assess their origin.

Evolution of placer PGM from the rocks

The source rock PGM assemblage is represented by those listed in Tarkian and Prichard (1987) and Prichard and Tarkian (1988), and it is also described in Prichard *et al*. (1986, 1988, 1994, 2017). Estimation of the percentages of each type of PGM given in Tables 1 and 2 and in Fig. 4*a*, is illustrative and for comparison purposes only. Prichard *et al*. (1994) also observed oxidized Pt and Pd phases in the chromite-rich rocks at Cliff. More recently, an extensive study of the PGM was carried out to find Os-bearing minerals for Os isotope analysis (e.g. Prichard *et al*., 2017). This revealed, in addition to those PGM already described, significant oxidation of the PGM including oxidized Pt–Pd–Ni–Cu-alloys and sperrylite. One grain of Pd–O, 60 μm in diameter, was also located. There is also the occurrence of breithauptite (NiSb) containing ~1% Pd as well as geversite ($PtSb_2$), Pt–Fe alloy and one Pd–Te–Sb–Bi (Fig. 13*c–f*). In the more recent survey it became clear that many of the laurite and clusters of PPGM grains have sizes in the rocks of 30–40 μm, reaching up to 60 μm.

https://doi.org/10.1180/minmag.2017.081.099 Published online by Cambridge University Press

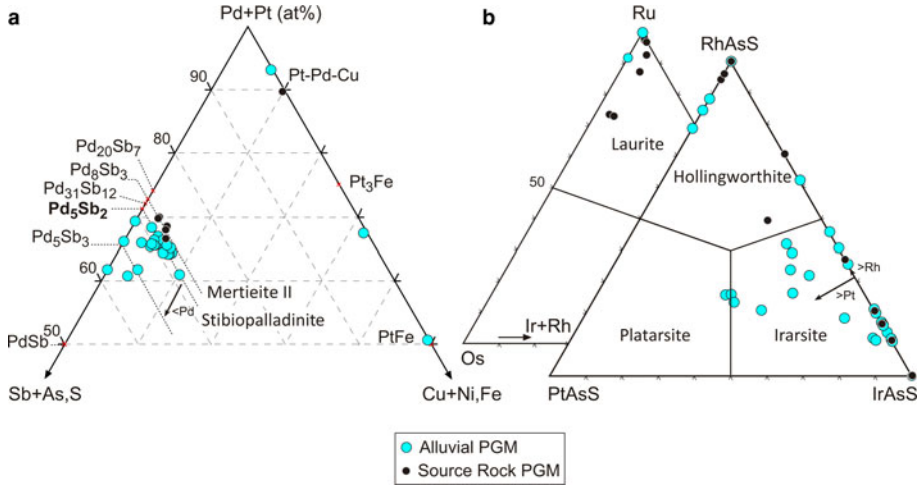

FIG. 10. Ternary diagrams (at.%) showing the composition of PGM from chromitites *vs.* streams at Cliff, Shetland ophiolite complex. (*a*) Pd–Sb–Cu ternary plot showing the composition of Pd-antimonides and Pt-alloys. Ideal phases within the Pd–Sb system are those reported by Kim and Chao (1991). (*b*) Ru–Os–Ir and Rh–Pt–Ir ternary plots showing the composition of laurite and sulfarsenides, respectively.

Cliff

The placer PGM assemblage recovered at Cliff reflects the type and abundance of those PGM in the rocks but there is less variety in the alluvial concentrates (Fig. 4*a*). Alluvial PGM are equally dominated by sperrylite, Pd-antimonides and sulfarsenides. In addition, Pd-sulfides, Pd-arsenide, platarsite and ruarsite (totalling 8 grains only) were also recovered from the streams. Millerite and nickeline are barren of PGE and occur only as internal inclusions in sperrylite. Scarce Pt-alloys (Pt–Pd–Cu, Pt–Fe) and laurite complete the alluvial PGM assemblage. Electrum and Cu–Pt- and Pd-bearing gold also occur as both single grains and coatings on detrital PGM. Alluvial PGM and associated gold have average sizes of 21 μm × 76 μm, and range from 5 to 110 μm in diameter.

Compared with the source rocks, there is a clear increase in sperrylite (>24%) and decrease in stibiopalladinite (<10%), irarsite and hollingworthite (<7%), and Pt-alloys (<2%) in the streams. Composite PGM of sperrylite with Pd-antimonide, irarsite and laurite occur in both the source rocks and placers. Laurite is equally scarce in rocks and streams (Fig. 4). The least abundant PGM in the rocks such as native Os, Rh–Sb–S, geversite ($PtSb_2$), potarite (PdHg) or rare Pd–Te phases are absent in the streams. Nickel- and Cu-bearing phases in the rocks such as ruthenian pentlandite, hongshiite (PtCu), Ni–Cu alloys and native Cu, have not been located in the alluvial concentrates either. Likewise, oxidized Pt- and Pd-phases are absent in the streams.

The composition of the common PGM between rocks and streams is rather similar, although some alluvial PGM such as irarsite, hollingworthite and Pt-alloys exhibit increase Pt contents while alluvial Pd-antimonides show a progressive loss of Pd. Increased Rh content is also observed in alluvial irarsite (Fig. 10*a*,*b*). Gold-bearing particles have a similar composition (Au–Pd, Au–Cu–Pt), although electrum dominates the alluvial assemblage.

Placer PGM are concentrated mainly where the stream meanders have formed, from which 58% of the PGM found were recovered (Fig. 4*b*). Only one grain of laurite was located towards the basal thrust. At this point the slope gradient and the water flow are intense, forming a waterfall under which loose sediment is deposited (Fig. 3*e*) and where a greater accumulation of heavy minerals is expected. Thus, it is clear that a great part of the alluvial PGM has been concentrated close to the quarries, particularly in the suitable meander zone, but PGM have not been able to travel further downstream.

The types of placer PGM do not vary significantly downstream. The most abundant PGM persist throughout the stream and have similar sizes. However, the shape of the alluvial PGM does vary and the PGM often show signs of disintegration downstream. Sperrylite and Pd-antimonides

https://doi.org/10.1180/minmag.2017.081.099 Published online by Cambridge University Press

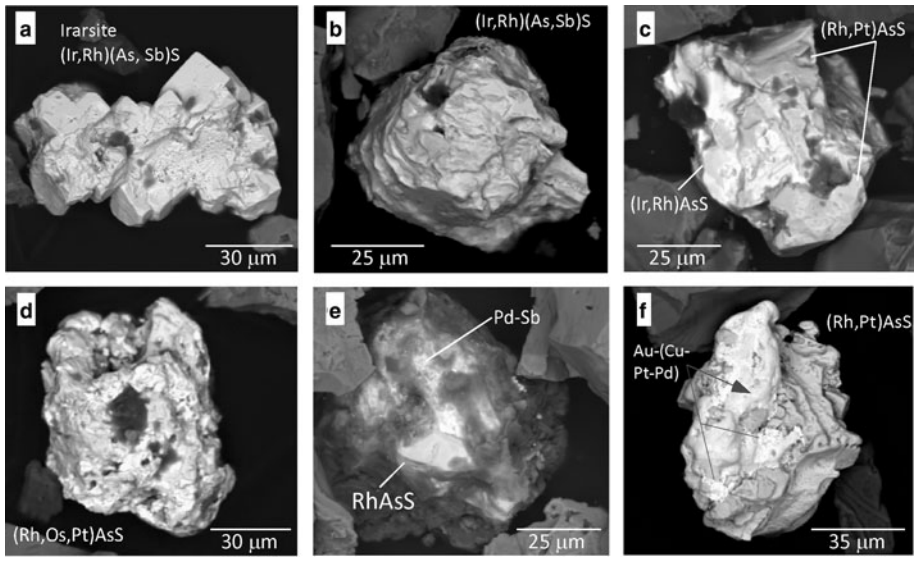

FIG. 11. Back-scattered electron images of sulfarsenides located in the streams from Cliff. (*a*) Aggregate of irarsite (IrAsS) grains with altered and pitted surface. (*b*) Single grain of irarsite with an etched appearance. (*c*) The only composite grain of irarsite and hollingworthite (RhAsS) found in the streams. Hollingworthite surrounds irarsite in the core. (*d*) Single grain of hollingworthite, subhedral and largely altered on surface. (*e*) Composite grain of hollingworthite and Pd-antimonide. (*f*) Composite grain of hollingworthite and a subhedral Cu–Pt–Pd-bearing particle of gold.

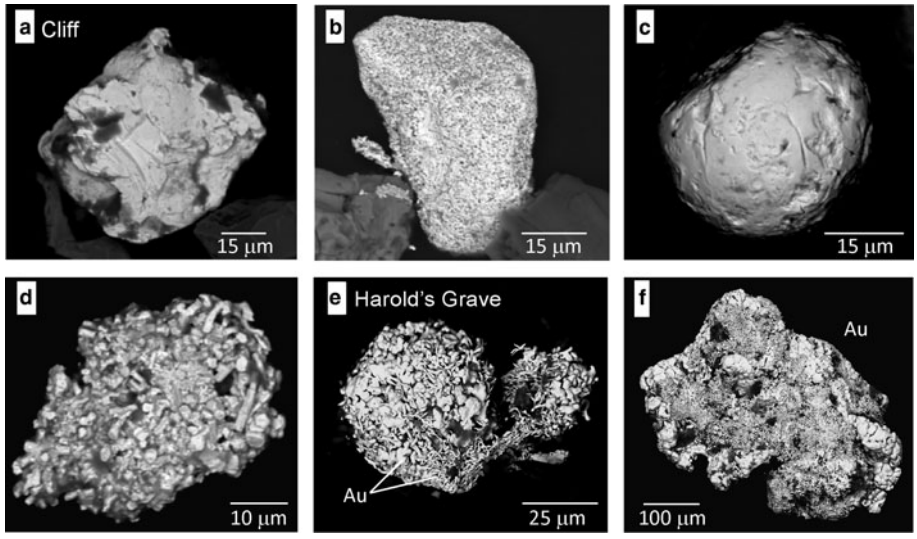

FIG. 12. Back-scattered electron images of gold grains in the stream from Cliff (*a–d*) and from Harold's Grave (*e–f*). (*a*) Irregular grain of electrum located close to the Cliff quarries. (*b*) Subhedral grain of pure gold with a very pitted surface located downstream, in the meander zone. (*c*) Rounded and polished grain of electrum downstream. (*d*) Porous grain of electrum with a delicate texture. (*e*, *f*) Globular grains of pure gold from the alluvial sands at Harold's Grave.

https://doi.org/10.1180/minmag.2017.081.099 Published online by Cambridge University Press

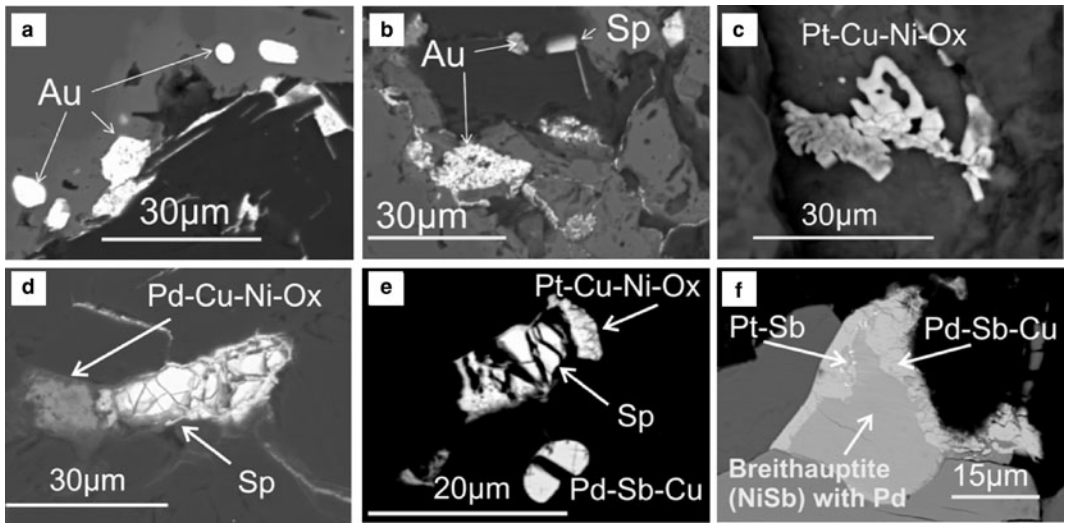

FIG. 13. Back-scattered electron images of gold and rare PGM in the source rocks. (*a*, *b*) Rounded porous primary Au, similar to the detrital electrum found in the placers. (*c*) Pt-Cu-Ni oxidized phase. (*d*) Pd-Cu-Ni oxidized phase on the edge of sperrylite and in stringers extending from the sperrylite. (*e*) Sperrylite and Pd antimonide with Cu both broken by chlorite laths. Sperrylite is partially altered to a Pt-Cu-Ni-oxide. (*f*) Breithauptite (NiSb) containing ~1% Pd coated on the edge by Pd antimonide which contains a small grain of geversite (Pt–Sb). These altered PGE-bearing phases (*c–f*) are all absent in the placer assemblage.

exhibit these variations most clearly as they are the most common PGM observed. Sperrylite, where it occurs close to the source rocks, retains its euhedral and angular form (Fig. 5) whereas further downstream it shows smoother surfaces and becomes progressively more rounded (Fig. 6). Pd-antimonides, where they are observed close to the quarries, are subhedral and have silicates attached to their surfaces whereas in the meander zone, these silicates are absent and the PGM may show lamellar structures. Further downstream, etching of Pd-antimonides is common in the form of concave faces or irregular surfaces (Fig. 9). The same is observed for Pd-sulfides, which are euhedral close to the quarries but appear broken down in the meander zone. Also for Pt-alloys, which are enclosed by other PGM close to the source rocks but appear as single, subrounded Pt–Fe particles downstream.

Harold's Grave

At Harold's Grave, PGM are dominated by IPGM (Tarkian and Prichard, 1987; Prichard *et al*., 1988, 2017). The IPGM assemblage in the rocks (Table 2) consists of laurite, osmium, irarsite and IrSbS. The size of the IPGM in the rocks ranges from a few micrometres to 500 μm, as found by Badanina *et al*. (2013, 2016) from concentrates of the rocks produced using the hydroseparation technique, and by Prichard *et al*. (2017) using 3D X-ray tomography. The PPGM are hollingworthite and scarce hongshiite (PtCu), Pt-alloy (Pt–Pd–Cu), genkinite and Pd-, Rh- and Ni-bearing antimonides totalling 9 grains only (<10%; Table 2). The survey by Prichard *et al*. (2017) corroborates that PPGM, including minor sperrylite, Pt–Fe alloys and platarsite, typically occur in clusters with Ru-pentlandite and some IPGM interstitially to chromite grains.

The placer PGM located at Harold's Grave ($n = 3$ grains) consist of laurite, iridium alloy and osmium alloy, with sizes ranging from 20 μm to 60 μm. No PPGM or pentlandite were recovered (Table 2). Despite the scarce PGM recovered, these represent the most abundant PGM in the IPGE-rich chromitites at Harold's Grave. The presence of gold is noteworthy. Detrital grains of Au–Cu have been detected but electrum and native Au also occur in porous aggregates up to 400 μm across with dendritic growths of native Au on surface. The sizes of the alluvial PGM and Au at Harold's Grave are in the range of those in the source rocks. No other statistically significant conclusions can be drawn due the low recovery of placer PGM in the panned samples.

https://doi.org/10.1180/minmag.2017.081.099 Published online by Cambridge University Press

Modification of PGM and PGE mobility

Overall, only slight differences are observed between the PGM assemblages of the rocks and streams:

(1) Those PGM enclosed by or in the edges of chromite grains in the source rocks are poorly represented or absent in the streams, suggesting that they may remain protected by their host minerals in the alluvial sands. This is mainly the case for Ru- and Os-PGM (laurite, osmium) within chromite grains in the rocks. Potarite (PdHg) also occurs in chromite, and antimonides (RhSbS, IrSbS, Rh–Ni–Sb, NiSb, Pd–Cu–Sb and genkinite) are often located in clusters within irarsite (Tarkian and Prichard, 1987; Prichard and Tarkian, 1988). The lack of these PGM in the streams is more evident at Harold's Grave, where the source chromitites are IPGE-enriched. In this case, however, the small dense fraction recovered may reflect lower erosion and a more restricted liberation of the host minerals and PGM into the streams.

(2) PGM that occur in the silicate matrix interstitial to chromite grains in the rocks, less protected against weathering, are largely represented in the streams at Cliff. These are sperrylite, stibiopalladinite, irarsite–hollingworthite–platarsite and Pt-alloys. Of these, sperrylite is the most resistant whereas Pd-, Ir-and Rh-PGM decrease in number and show slight changes in their composition (Figs 4, 10). Their abundance and composition suggest some progressive Pd-loss and Pt-gain in the streams. For example, alluvial stibiopalladinite grains extend towards Pd_5Sb_3 compositions and show a loss of up to 14 wt.% Pd. The alluvial Pt–Pd–Cu alloy contains less Pd (< 8 wt.%) and more Pt (>25 wt.%) than its counterpart in the rocks, and isoferroplatinum (Pt_3Fe) only occurs in the streams. Irarsite and hollingworthite also contain more Pt (>4%) in the streams than in the rocks (Fig. 10*b*).

(3) There are some losses of PGE-bearing phases from the rock assemblage into the streams. The most notable of these is the loss of all Pt and Pd oxides, which are poorly resistant compounds typically on the edges of broken PGM (Fig. 13*d–e*) that are not preserved during the transportation process. The disappearance of PGE-oxides or -hydroxides from source rocks in the fluvial environment has been reported previously from rivers draining the Great Dyke in Zimbawbe (Oberthür *et al*., 2003, 2013) and the Freetown layered complex in Sierra Leone (Bowles *et al*., 2017). Bowles *et al*. (2018) also noted the low stability of Cu-bearing sulfides and PGM such as tulameenite (Pt_2FeCu) during weathering of the rocks.

The low stability of Cu- and also Ni-bearing phases is also inferred from the eroded chromitites at the Shetland complex, as most of them (e.g. Ru-pentlandite, hongshiite PtCu and Cu-bearing alloys) are largely absent in the streams. All these phases occur in interstitial positions to chromite grains in the rocks. For example, hongshiite occurs at the edge of sperrylite and intergrown with Ni–Cu alloys, while Pt–Pd–Au–Cu and Pd–Cu alloys occur in composite grains with native Cu (Tarkian and Prichard, 1987; Prichard and Tarkian, 1988). Of all these, only sperrylite and one Pt–Pd–Cu alloy in stibiopalladinite remain in the streams. It is worth noting that Cu-bearing phases are scarce in the source rocks (Table 2) and some of them could have been missed during preparation of the panned samples. However, Ni- and Cu-intermetallic compounds and sulfides, and moreover pentlandite, are highly unstable phases in supergene conditions, and Ni and Cu can be lixiviated in a wide range of oxidizing Eh and acid to neutral pH conditions (Garrels and Christ, 1965; Williams, 1990; Takeno, 2005). Thus, Cu-bearing PGM from the Shetland chromitites, if not protected by their host (e.g. Fig. 8*a*,*d*; Fig. 9*e*), may have been destroyed during weathering.

(4) The textures and composition of the gold grains (Au–Pd, Au–Cu) in the rocks almost exactly mimic those in the placers with both rounded grains and spongy textured grains observed (Fig. 13*a*,*b*). They are clearly an integral part of the precious-metal occurrence at Cliff as they are located in the rocks and have not been derived from carriage by e.g. boulder clay from outside the area. Only dendritic growths of pure Au over Au-(Ag) grains at Harold's Grave may reflect some remobilization of Au at the grain scale (Fig. 12*e–f*). These particles satisfy the model for secondary Au formation described in Hough *et al*. (2011), which integrates a primary origin of the Au grains with secondary mobilization and aggregation processes on grains surfaces. This secondary Au typically displays high purity, very fine crystallinity, and a wide variety of morphologies, resulting from Au/Ag dissolution and Au precipitation acting simultaneously on the surface of the grains.

Although it is difficult to evaluate the metal mobility based on mineralogical observations alone, these data suggest that there is a preferential mobility of Pd, Cu, Ni and some Au over other metals (i.e. Pt, Rh, Ir, Os, Ru) in the secondary environment of the Shetland ophiolite complex.

https://doi.org/10.1180/minmag.2017.081.099 Published online by Cambridge University Press

Origin of the PGM

The overall similarity of the PGM assemblages of the PGE-rich rocks and the associated streams suggests that the PGM have weathered from the rock and their short transport distances have allowed them to preserve largely their compositions and often euhedral shapes. There are some losses from the rock assemblage, but the PGM assemblage in the rocks is very similar to that in the streams. The PGM in the streams are of a similar size to the larger PGM in the rocks reflecting a mechanical transportation process rather than a growth *in situ* of the PGM. This suggests early stages of dispersal of the PGE from the quarries.

The long-standing debate concerning the mechanical erosion of PGM from the source rocks versus the growth of PGM *in situ* downstream of the source has been a point of controversy for years. The sometimes contrasting mineralogical assemblages and PGM composition between sources and placers, the delicate morphologies and larger size of placer nuggets compared to primary PGM in the rocks or their isotopic signatures, all have been used in discussion to support both models.

It is considered that placer PGM are normally primary and are mechanically eroded from the source rocks (e.g. Cabri *et al*., 1996; Weiser, 2002; and references therein). In some complexes they may indeed be large PGM that are simply eroded from the rocks, as for example in some Ural-Alaskan type complexes. Some large PGM have been located in lode placers from the Nizhni Tagil and Kachkanar dunite massifs in the Uranium Platinum Belt, in the Vetnaya-Vyvenka Belt of Kamchatka, Russian Far East, or in the dunite core of the Pt-rich Alto Condoto Complex in Colombia (Weiser, 2002 and references therein). Rare, large PGM also occur in the oxidized Main Sulfide Zone of the Great Dyke, Zimbabwe (Oberthür *et al*., 2003) and also in the Shetland chromitites (Badanina *et al*., 2013).

Doubt was cast when Ottemann and Augustithis (1967) proposed that polyphase Pt–Fe nuggets in a laterite capping the massif of Yubdo (Ethiopia) formed at low temperatures by 'element agglutination'. Later, it was proposed that weathering of the rocks aided by organic acids in the soils alter and break down primary PGM liberating the PGE, which can be transported in solution through the soils down slope. Soils close to rivers or stream banks where Eh and pH conditions change allow for the precipitation of the PGE and the growth of PGM (Bowles, 1986; 1988; Bowles *et al*., 1994*a*,*b*, 1995). Selective metal leaching during weathering to form supergene PGM has been documented for the perfectly crystallized eluvial and alluvial PGM from the Freetown Igneous Complex, Sierra Leone (e.g. Bowles 1995; Bowles *et al*., 2013, 2017, 2018). Also for the oxidized Main Sulfide Zone of the Great Dyke, Zimbabwe and associated Pt-dominated alluvials (Oberthür *et al*., 2003), as well as for the botryoidal and arborescent Pt–Pd aggregates and the Pt-enriched rims on detrital PGE-alloys from the Bom Succeso stream in Minas Gerais, Brazil (Cabral *et al*., 2007, 2009).

There are many other examples of PGE-bearing phases that apparently formed in low temperature conditions (~100–25°C) in varied deposits. One example are the internally zoned Au–Pd arborescent grains from Hope's Nose, UK (Leake *et al*., 1991) and Serra do Espinhaço, Minas Gerais (Cabral *et al.*, 2008). Another example are the rosettes of native Pd on the surface of gold nuggets from Gongo Soco Fe-ores, Minas Gerais (Cabral and Kwitko-Ribeiro, 2004) and the Pd–Cu rosettes coating goethite in the Limoeiro Ni–Cu–(PGE) deposit (Mota-e-Silva *et al*., 2016). Neoformed Pt–Ir–Fe–Ni alloys and layers of Ir-rich alloys on multistage PGE-grains are reported from Ni-laterites in the Falcondo mining area, Dominican Republic (Aiglsperger *et al*., 2016). It appears that supergene precipitation of PGE could be aided by both biogenic activity (Reith *et al*., 2016; Bowles *et al*., 2018) and inorganic processes such as bioreduction or electrochemical accretion of metals (e.g. Cabral *et al*., 2011; Aiglsperger *et al*., 2016).

The resolution to this controversy may be partially explained in that both ideas are correct in certain circumstances. Mechanical erosion may be more prominent in high latitudes where mechanical erosion dominates over chemical weathering. However, in tropical conditions, chemical weathering dominates and PGM may precipitate *in situ*, perhaps in soils or stream banks distally to the source rocks following the chemical disintegration of the primary PGM. Rock-weathering conditions in humid and temperate zones, with high rainfall and abundant organic material would enhance PGE mobility and redeposition. It is clear that both primary (magmatic or hydrothermally modified) PGM mechanically liberated from the rocks and secondary, reworked or neoformed supergene PGE-bearing minerals, can coexist in some eluvial and alluvial placers.

In the Shetland Islands mechanical erosion dominates and is operating only on a small scale very close to the source. The PGM in the streams

https://doi.org/10.1180/minmag.2017.081.099 Published online by Cambridge University Press

reflect the source rocks as they are very close to them. There are signs of disintegration of the PGM as they travel downstream. Pd-antimonides weather to produce furrowed surfaces and concave etched surfaces whereas sperrylite starts with jagged edges that become rounded downstream. The greater initial disintegration of Pd-bearing phases over sperrylite observed at Cliff may be a result of the greater mobility of Pd over Pt which has been consistently observed, including in surficial weathering environments (e.g. Fuchs and Rose, 1974; Wood and Vlassopoulos, 1990; Prichard and Lord, 1994; Salpéteur *et al*., 1995; Prichard *et al*., 2001; Suárez *et al*., 2010, Bowles *et al*., 2013). Sperrylite is harder than Pd-antimonides and has proved to be considerably more durable and resistant to weathering and mechanical erosion (e.g. Oberthür *et al*., 2003, 2013; Suárez *et al*., 2010), which also appears true in this study of placer PGM at the Shetlands ophiolites.

Conclusions

The PGM assemblage in the streams at Cliff consists dominantly of sperrylite and Pd-antimonides and this is reflected by the PGM found in the rocks. The extreme proximity of the source to the streams and the well documented PGM assemblage in the rocks allows a comparison of PGM compositions and sizes in the rocks against those in the streams. This reveals that the assemblages are very similar although there are notable absences of some PGM types in the streams. The Pt and Pd oxides in the rocks are missing in the streams, demonstrating that they are very fragile and unlikely to survive erosion. Nickle sulfides and Cu-bearing PGM and alloys are also unstable phases that remain in the streams only when protected by their original host minerals. Thus there is a continuum from magmatic formation and hydrothermal upgrading of the PGM assemblage in the rocks through to initial weathering and oxidation of the PGM in the rocks through to erosion into the streams. Within the streams there is further evidence of change in the PGM assemblage. More resistant minerals such as sperrylite persist downstream becoming more rounded whereas Pd antimonides can be observed in the early stages of disintegration with concave etching on their surfaces. Laurite and members of the irarsite–hollingworthite–platarsite solid-solution series are also preserved in the streams. The common Pt–Fe alloys observed in many placer deposits are largely absent. The gold grains in the streams are eroded from the Cliff assemblage in the rocks as indicated by the close similarity of the textures that they show in both the rocks and in the streams. The presence of Au–Pd and Au–Cu layers over primary PGM and of native Au in dendritic growths may indicate a local remobilization of these elements in surface conditions, at least on the grain scale. Otherwise the PGM assemblage preserved in the streams at Cliff is early stage with PGM having been mechanically eroded from the nearby source rocks and there is no evidence of growth *in situ* of PGM in the placers rather mechanical disintegration. This is early stage mechanical erosion and so the usual Os–Ir–Ru alloys that characterizes ophiolitic placer PGM are not present. This is more evident at Harold's Grave, where the few IPGM found in the streams reflect the restricted release of the PGM enclosed by primary minerals in the source rocks. In general, the alluvial PGM assemblage found in the streams draining the Shetland complex mimics the rather unusual suite of PGM in the PGE-rich ophiolitic rocks.

Acknowledgements

We would like to thank The Department of Education, Universities and Research of the Basque Government (Refs. IT762-13, BFI-2011-254) for additional funding and Dr. R.S. Garcia (UPV/EHU) for her technical support. We also thank the helpful comments by Dr. F. Zaccarini and another anonymous referee, which greatly improved the quality of the manuscript, and Drs. B. O'Driscoll and I. McDonald for the editorial handling. The coauthors of this work are very grateful to D.R. Sharp, A. Colling and Dr. J.F.W. Bowles for their contributions to this manuscript. We dedicate this work with all of our love to Prof. Hazel M. Prichard and John S. Watson.

References

Aiglsperger, T., Proenza, J.A., Font-Bardia, M., Baurier-Aymat, S., Galí, S., Lewis, J.F. and Longo, F. (2016). Supergene neoformation of Pt-Ir-Fe-Ni alloys: multi-stage grains explain nugget formation in laterites. *Mineralium Deposita*, **52**, 1069–1083.

Augé, T., Legendre, O. and Maurizot, P. (1998) The distribution of Pt and Ru-Os-Ir minerals in the New Caledonia ophiolite. Pp. 141–154 in: *International Platinum* (P.N. Laverov and V.V. Distler, editors). Theophrastus publications, St. Petersburg, Athens.

Bacuta, G.C.J., Lipin, B.R., Gibbs, A.K. and Kay, R.W. (1988) Platinum-group element abundance in

https://doi.org/10.1180/minmag.2017.081.099 Published online by Cambridge University Press

chromite deposits of the Acoje ophiolite block, Zambales ophiolite complex, Philippines. Pp. 381–382 in: *Geo-Platinum Symposium Volume* (H. M. Prichard, P.J. Potts, J.F.W. Bowles and S.J. Cribb, editors). Elsevier.

Badanina, I.Y., Malitch, K.N., Lord, R.A. and Meisel, T.C. (2013) Origin of primary assemblage in chromitite from a mantle tectonite at Harold's Grave (Shetland Ophiolite Complex, Scotland). *Mineralogy and Petrology*, **107**, 963–970.

Badanina, I.Y., Malitch, K.N., Lord, R.A., Belousova, E. A. and Meisel, T.C. (2016) Closed-system behaviour of the Re–Os isotope system recorded in primary and secondary platinum-group mineral assemblages: evidence from a mantle chromitite at Harold's Grave (Shetland Ophiolite Complex,Scotland). *Ore Geology Reviews*, **75**, 174–185.

Bowles, J.F.W. (1986) The development of platinum-group minerals in laterites. *Economic Geology*, **81**, 1278–1285.

Bowles, J.F.W. (1988) Further studies of the development of platinum-group minerals in the laterites of the Freetown Layered Complex, Sierra Leone. Pp. 273–280 in: *Proceedings of the symposium Geo-Platinum 87*. (H.M. Prichard, P.J. Potts, J.F.W. Bowles and S.J. Cribb, editors). Elsevier Applied Science, London.

Bowles, J.F.W. (1995) The development of platinum-group minerals (PGM) in laterites: mineral morphology. *Chronique de la Recherche Minière*, **520**, 55–63.

Bowles, J.F.W., Giże, A.P. and Cowden, A. (1994*a*) The mobility of the platinum-group elements in the soils of the Freetown Peninsula, Sierra Leone. *The Canadian Mineralogist*, **32**, 957–967.

Bowles, J.F.W., Giże, A.P., Vaughan, D.J. and Norris, S.J. (1994*b*) The development of platinum-group minerals in laterites; an initial comparison of the organic and inorganic controls. *Transactions of the Institute of Mining and Metallurgy, B Applied Earth Science*, **103**, 53–56.

Bowles, J.F.W., Giże, A.P., Vaughan, D.J. and Norris, S.J. (1995) Organic controls on platinum-group element (PGE) solubility in soils: initial data. *Chronique de la Recherche Minière*, **520**, 65–73.

Bowles, J.F.W., Lyon, I.C., Saxton, J.M. and Vaughan, D. J. (2000) The origin of platinum group minerals from the Freetown Intrusion, Sierra Leone, inferred from osmium isotope systematics. *Economic Geology*, **95**, 539–548.

Bowles, J.F.W., Prichard, H. M., Suárez, S. and Fisher, P. C. (2013) The first report of platinum-group minerals in magnetite-bearing gabbro, Freetown layered Complex, Sierra Leone: occurrences and genesis. *The Canadian Mineralogist*, **51**, 455–473.

Bowles, J.F.W., Suárez, S., Prichard, H.M. and Fisher, P.C. (2017) Weathering of PGE sulfides and Pt–Fe alloys in the Freetown Layered Complex, Sierra Leona. *Mineralium Deposita*, **52**, 1127–1144.

Bowles, J.F.W., Suárez, S., Prichard, H.M. and Fisher, P.C. (2018) The mineralogy, geochemistry and genesis of the alluvial platinum-group minerals of the Freetown Layered Complex, Sierra Leone. *Mineralogical Magazine*, **82**(S1), S223–S246.

Bridges, J.C., Prichard, H.M., Neary, C.R. and Meireles, C. A. (1993) Platinum-group element mineralization in the chromite-rich rocks of the Braganca massif, northern Portugal. *Transactions Institute Mining Metallurgy, B Applied Earth Science*, **102**, 103–113.

Brough, C.P., Prichard, H.M., Neary, C.R., Fisher, P.C. and McDonald, I. (2015) Geochemical variations within podiform chromitite deposits in the Shetland Ophiolite: Implications for petrogenesis and PGE concentration. *Economic Geology*, **110**, 187–208.

Cabral, A.R. and Kwitko-Ribeiro, R. (2004) On the rossettes of "native palladium" from Minas Gerais, Brazil: evidence from Gongo Soco. *The Canadian Mineralogist*, **42**, 683–674.

Cabral, A.R., Beaudoin, G., Choquette, M., Lehmann, B. and Polônia, J.C. (2007) Supergene leaching and formation of platinum in alluvium: evidence from Serro, Minas Gerais, Brazil. *Mineralogy and Petrology*, **90**, 141–150.

Cabral, A.R., Tupinanbá, M., Lehmann, B., Kwitko-Ribeiro, R. and Vymazalová, A. (2008) Arborescent palladiniferous gold and empirical Au_2Pd and Au_3Pd in alluvium from southern Serra do Espinhaço, Brazil. *Neues Jahrbuch für Mineralogie Abhandlungen*, **148**/3, 329–336.

Cabral, A.R., Lehmann, B., Tupinambà, M., Schlosser, S., Kwitko-Ribeiro, R. and Abreu, F.R. (2009) The platiniferous Au-Pd belt of Minas Gerais, Brazil, and genesis of its botroidal Pt-Pd aggregates. *Economic Geology*, **104**, 1265–1276.

Cabral, A.R., Radtke, M., Munnik, F., Lehmann, B., Reinholz, U., Riesemeier, H., Tupinambá, M. and Kwitko-Ribeiro, R. (2011) Iodine in alluvial platinum–palladium nuggets: Evidence for biogenic precious-metal fixation. *Chemical Geology*, **281**, 125–132.

Cabri, L.J. and Harris, D.C. (1975) Zoning of Os-Ir alloys and the relation of the geological and tectonic environment of the source rocks to the bulk Pt:Pt+Ir+Os ratio for placers. *The Canadian Mineralogist*, **13**, 266–274.

Cabri, L.J., Harris, D.C. and Weiser, T.W. (1996) Mineralogy and petrology of platinum-group mineral (PGM) placer deposits of the world. *Exploration and Mining Geology*, **5**, 73–176.

Corrivaux, L. and Laflamme, J.H.G. (1990) Minéralogie des éléments du groupe du platine dans les chromitites de l'ophiolite de Thetford mines, Québec. *The Canadian Mineralogist*, **28**, 579–595.

https://doi.org/10.1180/minmag.2017.081.099 Published online by Cambridge University Press

Derbyshire, E.J., O'Driscoll, B., Lenaz, R., Gertisser, R. and Kronz, A. (2012) Compositionally heterogeneous podiform chromitite in the Shetland Ophiolite Complex (Scotland): Implications for chromitite petrogenesis and late stage alteration in the upper mantle portion of a supra-subduction zone ophiolite. *Lithos*, **162–163**, 279–300.

Escayola, M., Garuti, D., Zaccarini, F., Proenza, J., Bédard, J.H. and Van Staal, C. (2011) Chromitite and platinum-group-element mineralization at Middle Arm Brook, Central Advocate Ophiolite Complex, Baie Verte Peninsula, Newfoundland, Canada. *The Canadian Mineralogist*, **49**, 1523–1547.

Flinn, D. (1985) The Caledonides of Shetland. Pp. 1159–1172 in: *The Caledonide Orogeny – Scandinavia and Related Areas* (D.G. Gee and B.A. Sturt, editors.). John Wiley and Sons Ltd.

Fuchs, W.A. and Rose, A.W. (1974) The geochemical behavior of platinum and palladium in the weathering cycle in the Stillwater Complex, Montana. *Economic Geology*, **69**, 332–346.

Garrels, R.M. and Christ, C.L. (1965) *Solutions, Minerals, and Equilibria*. Harper & Row, Publishers, New York, 450 pp.

González-Jiménez, J.M., Griffin, W.L., Proenza, J.A., Gervilla, F., O'Reilly, S.Y., Akbulut, M., Pearson, N.J. and Arai, S. (2014). Chromitites in ophiolites: How, where, when, why? Part II. The crystallization of chromitites. *Lithos*, **189**, 140–158.

Grammatikopoulos, T.A., Kapsiotis, A., Zaccarini, F., Tsikouras, B., Hatzipanagiotou, K. and Garuti, G. (2007). Investigation of platinum-group minerals (PGM) from Pindos chromitites (Greece) using hydroseparation concentrates. *Minerals Engineering*, **20**, 1170–1178.

Hough, R., Noble, R. and Reich, M. (2011) Natural gold nanoparticles. *Ore Geology Review*, **42**, 55–61.

Kim, W.-S. and Chao, G.Y. (1991) Phase relations in the system Pd-Sb-Te. *The Canadian Mineralogist*, **29**, 401–409.

Kozlu, H., Prichard, H.M., Melcher, F., Fisher, P.C., Brough, C. and Stueben, D. (2014) Platinum group element (PGE) mineralisation and chromite geochemistry in the Berit ophiolite (Elbistan/Kahramanmaraş), SE Turkey. *Ore Geology Reviews*, **60**, 97–111.

Leake, R.C., Bland, D.J., Styles, M.T. and Cameron, D.G. (1991) Internal structure of Au-Pd-Pt grains from south Devon, England in relation to low temperature transport and deposition. *Transactions of the Institute of Mining and Metallurgy, B Applied Earth Science*, **100**, B159–178.

Lord, R.A., Prichard, H.M. and Neary, C.R. (1994) Magmatic PGE concentrations and hydrothermal upgrading in the Shetland ophiolite complex. *Transactions Institute Mining Metallurgy, B Applied Earth Science*, **103**, B87–162.

Moreno, T., Prichard, H., Lunar, R., Monterrubio, S. and Fisher, P. (1999). Formation of a secondary platinum-group minerals assemblage in chromitites from the Herbeira ultramafic massif in Cabo Ortegal, NW Spain. *European Journal of Mineralogy*, **11**, 363–378.

Moreno, T., Gibbons, W., Prichard, H.M. and Lunar, R. (2001). Platiniferous chromitite and the tectonic setting of ultramafic rocks in Cabo Ortegal, NW Spain. *Journal of the Geological Society*, **158**, 601–614.

Mota-e-Silva, J., Prichard, H.M., Suárez, S., Ferreira Filho, C.F. and Fisher, P.C. (2016) Supergene alteration of platinum-group minerals and the formation of Pd-Cu-O and Pd-I-O compounds in the Limoeiro Ni-Cu-(PGE) deposit, Brazil. *The Canadian Mineralogist*, **54**, 755–778.

Oberthür, T., Weiser, T.W. and Gast, L. (2003) Geochemistry and mineralogy of platinum-group elements at Hartley Platinum Mine, Zimbabwe Part 2. Supergene redistribution in the oxidized Main Sulfide Zone of the Great Dyke, and alluvial platinum group minerals. *Mineralium Deposita*, **38**, 344–355.

Oberthür, T., Weiser, T.W., Melcher, F., Gast, L. and Wöhrl, C. (2013) Detrital platinum-group minerals in rivers draining The Great Dyke, Zimbabwe. *The Canadian Mineralogist*, **51**, 197–222.

Ohnenstetter, M., Johan, Z., Coherie, A., Fouillac, A., Guerrot, C., Ohnenstetter, D., Chaussidon, M., Rouer, O., Makovicky, E., Makovicky, M., Rose-Hansen, J., Karup-Moller, S., Vaughan, D., Tumer, G., Pattrick, R.A.D., Gize, A.P., Lyon, I. and McDonald, I. (1999) New exploration methods for platinum and rhodium deposits poor in base-metal sulfides. *Transactions Institute Mining Metallurgy, B Applied Earth Science*, **108**, 119–150.

Orberger, B., Fredrich, G. and Woermann, E. (1988) Platinum-group element mineralisation in the ultramafic sequence of the Acoje ophiolite block, Zambales, Philippines. Pp. 391–380 in: *Geo-Platinum Symposium Volume* (H.M. Prichard, P.J. Potts, J.F.W. Bowles and S.J. Cribb, editors). Elsevier.

O'Driscoll, B. and González-Jiménez, J.M. (2016) Petrogenesis of the platinum-group minerals. Pp. 489–578 in: *Highly Siderophile and Strongly Chalcophile Elements in High-Temperature Geochemistry and Cosmochemistry*, (J. Harvey and J. M.D. Day, editors). Reviews in Mineralogy & Geochemistry, **81**. Mineralogical Society of America and the Geochemical Society, Chantilly, Virginia, USA.

Ottemann, J. and Augustithis, S.S. (1967) Geochemistry and Origin of "Platinum-Nuggets" in Lateritic Covers from Ultrabasic Rocks and Birbirites of W. Ethiopia. *Mineralium Deposita*, **1**, 269–277.

Pedersen, R.B., Johannesen, G.M. and Boyd, R. (1993) Stratiform PGE mineralisations in the ultramafic cumulates of the Leka ophiolite complex, central Norway. *Economic Geology*, **88**, 782–803.

https://doi.org/10.1180/minmag.2017.081.099 Published online by Cambridge University Press

Prichard, H.M. (1985) The Shetland Ophiolite. Pp 1173–1184 in: *The Caledonide Orogeny – Scandinavia and Related Areas* (D.G. Gee and B.A. Sturt, editors.). John Wiley and Sons Ltd.

Prichard, H.M. and Brough, C.P. (2009) Potential of ophiolite complexes to host PGE deposits. Pp. 277–290 in: *New Developments in Magmatic Ni-Cu and PGE Deposits* (C. Li and E.M. Ripley, editors.). Geological Publishing House, Beijing.

Prichard, H.M. and Lord, R.A. (1993) An overview of the PGE concentrations in the Shetland ophiolite complex. Pp. 273–294 in: *Magmatic Processes and Plate Tectonics* (H.M. Prichard, T. Alabaster, N.B. Harris, C.R. Neary, editors). **Vol. 76**, Geological Society of London.

Prichard, H.M. and Lord, R.A. (1994) Evidence for the mobility of PGE in the secondary environment in the Shetland ophiolite complex. *Transactions Institute Mining Metallurgy, B Applied Earth Science*, **103**, 79–86.

Prichard, H.M. and Tarkian, M. (1988) Platinum and palladium minerals from two PGE-rich localities in the Shetland Ophiolite Complex. *The Canadian Mineralogist*, **26**, 979–990.

Prichard, H.M., Neary, C.R. and Potts, P.J. (1986) Platinum-group minerals in the Shetland Ophiolite. Pp. 395–414 in: *Metallogeny of the Basic and Ultrabasic Rocks* (M.J. Gallagher, R.A. Ixer, C.R. Neary and H.M. Prichard, editors). Transactions Institute Mining Metallurgy.

Prichard, H.M., Potts, P.J., Neary, C.R., Lord, R.A. and Ward, G.R. (1988) *Development of techniques for the determination of the platinum-group elements in ultramafic rock complexes of potential economic significance: mineralogical studies*. Commission of the European Communities. Report EUR 11631, 163 pp. ISBN 92-825-9245-6.

Prichard, H.M., Ixer, R.A., Lord, R.A., Maynard, J. and Williams, N. (1994) Assemblages of platinum-group minerals and sulfides in silicate lithologies and chromite-rich rocks within the Shetland Ophiolite. *The Canadian Mineralogist*, **32**, 271–294.

Prichard, H.M., Sá, J.H.S. and Fisher, P.C. (2001) Platinum-group mineral assemblages and chromite composition in the altered and deformed Bacuri complex, Amapa, North Eastern Brazil. *The Canadian Mineralogist*, **39**, 377–396.

Prichard, H.M., Economou-Eliopoulos, M. and Fisher, P. C. (2008*a*) Platinum-group minerals in podiform chromitite in the Pindos ophiolite complex, Greece. *The Canadian Mineralogist*, **46**, 329–341.

Prichard, H.M., Neary, C.R., Fisher, P.C. and O'Hara, M. J. (2008*b*) PGE-rich podiform chromitites in the Al'Ays Ophiolite complex, Saudi Arabia: An example of critical mantle melting to extract and concentrate PGE. *Economic Geology*, **103**, 1507–1529.

Prichard, H.M., Barnes, S.J., Dale, C.W., Godel, B., Fisher, P.C. and Nowell, G.M. (2017) Paragenesis of multiple platinum-group mineral populations in Shetland ophiolite chromitite: 3D X-ray tomography and in situ Os isotopes. *Geochimica et Cosmochimica Acta*, **216**, 314–334.

Reith, F., Zammit, C.M., Shar, S.S., Etschmann, B., Bottrill, R., Southam, G., Ta, C., Kilburn, M., Oberthür, T., Bail, A.S. and Brugger, J. (2016) Biological role in the transformation of platinum group mineral grains. *Nature Geoscience*, **9**, 294–298.

Salpéteur, I., Martel-Jantin, B. and Rakotomanana, D. (1995) Pt and Pd mobility in ferralitic soils of the West Andriamena area (Magadascar). *Evidence of a supergene origin of some Pt and Pd minerals*. Chronique de la Recherche Minière, **520**, 27–45.

Suárez, S., Prichard, H.M, Velasco, F., Fisher, P.C. and McDonald, I. (2010) Alteration of platinum-group minerals and dispersion of platinum-group elements during progressive weathering of the Aguablanca Ni-Cu deposit (SW Spain). *Mineralium Deposita*, **45**, 331–350.

Takeno, N. (2005) *Atlas of Eh-pH diagrams. Intercomparison of thermodynamic databases*. Geological Survey of Japan Open File Report No.419, 287 p.

Tarkian, M. and Prichard, H.M. (1987) Irarsite-hollingworthite solid-solution series and other associated Ru-, Os-, Ir-, and Rh bearing PGM's from the Shetland Ophiolite Complex. *Mineralium Deposita*, **22**, 178–184.

Weiser, T.W. (2002) Platinum-group minerals (PGM) in placer deposits. Pp. 721–756 in: *The Geology, Geochemistry, Mineralogy and Mineral Beneficiation of Platinum-Group Elements*. (L.J. Cabri, editor). Canadian Institute of Mining, Metallurgy and Petroleum, special volume 54.

Williams, P.A. (1990) *Oxide Zone Geochemistry.* Ellis Horwood Series in Inorganic Chemistry, 286 pp.

Wood, S.A. and Vlassopoulos, D. (1990) The dispersion of Pt, Pd, and Au in surficial media about two PGE-Cu-Ni prospects in Quebec. *The Canadian Mineralogist*, **28**, 649–663.

Zaccarini, F., Pushkarev, E., Garuti, G., Krause, J., Dvornik, G.P., Stanley, C. and Bindi, L. (2013) Platinum group minerals (PGM) nuggets from alluvial-eluvial placer deposits in the concentrically zoned mafic-ultramafic Uktus complex (Central Urals, Russia). *European Journal of Mineralogy*, **25**, 519–531.

https://doi.org/10.1180/minmag.2017.081.099 Published online by Cambridge University Press